AD NUMBER

AD253484

LIMITATION CHANGES

TO:

Approved for public release; distribution is unlimited.

FROM:

**Distribution authorized to U.S. Gov't. agencies and their contractors;
Administrative/Operational Use; 31 AUG 1960.
Other requests shall be referred to Army Signal Research and Development Laboratory, Fort Monmouth, NJ.**

AUTHORITY

ECOM ltr dtd 5 May 1971

MISSING PAGE
NUMBERS ARE BLANK
AND WERE NOT
FILMED

290 400

FINAL REPORT INVESTIGATION OF COMPOSITE OR STACKED VARIABLE ENERGY GAP PHOTOVOLTAIC SOLAR ENERGY CONVERTER

Prepared for Commanding Officer, U.S. ARMY SIGNAL RESEARCH AND DEVELOPMENT LABORATORY, Fort Monmouth, New Jersey

Contract DA 36-039 SC 85244

1 September 1959 to 31 August 1960

EOS Report 400-Final

The work performed in this contract was made possible by the support of ARPA under Order No. 80-59 through the USASRDL.

EOS ELECTRO-OPTICAL SYSTEMS, INC., Pasadena, California

Copy No 34

FINAL REPORT INVESTIGATION OF COMPOSITE OR STACKED VARIABLE ENERGY GAP PHOTOVOLTAIC SOLAR ENERGY CONVERTER

Prepared for Commanding Officer, U.S. ARMY SIGNAL RESEARCH AND DEVELOPMENT LABORATORY, Fort Monmouth, New Jersey

Contract DA 36-039 SC 85244
1 September 1959 to 31 August 1960

EOS Report 400-Final

The work performed in this contract was made possible by the support of ARPA under Order No. 80-59 through the USASRDL.

The object of this research is the attainment of improved photovoltaic solar energy conversion efficiency by means of improved composite photovoltaic solar energy converters.

Prepared by
James W. Burns
J. W. Burns
Project Supervisor

Approved by
W V Wright
W. V. Wright, Manager
Solid State Division

E O S
ELECTRO-OPTICAL SYSTEMS, INC., Pasadena, California

CONTENTS

CONTENTS (cont)

ILLUSTRATIONS

Figure

Table

1. PURPOSE

The study of composite solar cells was directed toward the attainment of improved photovoltaic solar energy conversion efficiency by improvement of the spectral efficiency of the device. The primary objective of the work was the demonstration of the feasibility of improved efficiency composite energy gap cells.

The program was divided into three parts, as follows:

1. The carrying through of a thorough analytical investigation of the composite photovoltaic solar energy converter. This investigation was to lead to recommendations for the optimum semiconductor materials to be utilized in the composite converter, and to recommendations for the design configuration.

2. The preparation and acquisition of semiconductor materials for the composite converter.

3. The fabrication and evaluation of experimental composite photovoltaic solar energy converters. These were to be fabricated from the semiconductor materials which would optimize the energy conversion process, and the design was to be directed toward the achievement of 20 percent conversion efficiency.

2. ABSTRACT

A theoretical analysis is given of the performance of composite photovoltaic solar energy converters consisting of two separate p-n junction cells of differing energy gaps. The analysis considers the spectral efficiencies of the separate cells and the effects of saturation currents as a function of energy gaps. The failure of the forward current to vary as rapidly as exp (qV/kT) is discussed on the basis of non-radiative recombinations in the space charge layer. The effect of such recombinations on cell efficiency is analyzed, and graphs of efficiency vs. energy gaps in the composite cell are given for the ideal case of no non-radiative recombinations and for several recombination rates. For the ideal case the optimum energy gaps are found to be 1.1 eV and 1.65 eV, and the maximum efficiency 32.5 percent. The optimum energy gaps increase with a departure from the ideal, and the maximum efficiency decreases. A correlation is drawn between the efficiency of carrier collection and the effect of diffused layer resistance, and it is found that the optimum junction depth in a solar cell is approximately one-fourth of the minority carrier diffusion length.

On the basis of the analysis, Si is chosen for the lower-energy-gap component of the composite cell, and AlSb and CdSe are selected as possible materials for the higher-energy-gap component. The purification of Al and the growth of crystals of AlSb are described in detail. A description is also given of the preparation of crystals of CdSe, but neither AlSb nor CdSe were prepared with sufficient purity to warrant solar cell fabrication.

The results of measurements in sunlight of the power output of a composite cell in which Si and CdS form the active elements are given. As expected, these results indicate that CdS is not one of the optimum materials for a composite solar cell.

3. PUBLICATIONS, LECTURES, REPORTS, AND CONFERENCES

3.1 Publications

No direct publications resulted from the research and development carried out under this contract. A report on the work was included in a paper given by W. Cherry, USASRDL, on the progress being made in the ARPA solar energy conversion program. This paper was presented at the 14th Annual Power Sources Conference in Atlantic City, May, 1960.

3.2 Lectures

No lectures based on the subject efforts were given.

3.3 Reports

The following progress reports were submitted, under the title "Investigation of Composite or Stacked Variable Energy Gap Photovoltaic Solar Energy Converter":

Report Number	Date	Authors
EOS Report No. 400-M-1	1 October 1959	J. W. Burns
" " " 400-M-2	1 November 1959	J. W. Burns
" " " 400-M-3	1 December 1959	J. W. Burns, W. H. Evans
" " " 400-M-4	1 January 1960	J. W. Burns
" " " 400-2Q-1	8 January 1960	J. W. Burns, W. H. Evans and H. Armstrong
" " " 400-M-5	1 February 1960	J. W. Burns, W. H. Evans
" " " 400-M-6	1 March 1960	J. W. Burns
" " " 400-M-7	1 April 1960	J. W. Burns
" " " 400-M-8	1 May 1960	J. W. Burns
" " " 400-M-9	1 June 1960	J. W. Burns
" " " 400-M-10	1 July 1960	J. W. Burns
" " " 400-2Q-2	10 July 1960	J. W. Burns, W. H. Evans
" " " 400-M-11	1 August 1960	J. W. Burns
" " " 400-M-12	1 September 1960	J. W. Burns

3.4 Conferences

The Project Supervisor, Mr. J. W. Burns, visited the Evans Signal Laboratory, Ft. Monmouth, N. J., on 11 and 12 February 1960, to review the work done to date with the USASRDL Technical Monitor, Mr. J. Mandelkorn, and to attend a joint meeting with representatives of USASRDL and the seven other contractors concomitantly engaged with Mr. W. Cherry's office in the ARPA program for solar energy conversion. The purpose of the joint meeting, held on 12 February 1960, was to have each representative give a short presentation of the work being done in his particular phase of the photovoltaic solar energy conversion program. The representatives stated the object of their work, the results obtained, the difficulties encountered, and the merits of the particular approach. The attendees at this meeting were:

William Cherry, USASRDL
Joseph Mandelkorn, USASRDL
James Kesperis, USASRDL
Emil Kittle, USASRDL
Robert Mark, USASRDL
George Hunrath, USASRDL
James W. Burns, Electro-Optical Systems, Inc.
Lewis Stone, Eagle-Picher Laboratories
Robert Robinson, Armour Research
John Buttrey, Armour Research
Gene Ralph, Hoffman Semiconductor Division
Paul Rappaport, RCA Laboratories
James Elliot, General Electric Company
Fred Fitch, Grace Chemical Company
Wayne Barrett, Grace Chemical Company
Pierre Lamond, Transitron Electronics

On 29 March 1960, it was our pleasure to be visited by Mr. James Kesperis of USASRDL. The progress and future directions of the effort were discussed, and it was decided that most of the effort in

the succeeding months should be devoted to AlSb and AlSb solar cells.

On 21 June 1960 the Project Supervisor visited Messrs. W. Cherry and J. Mandelkorn at the Evans Laboratory, Ft. Monmouth, N. J. It was agreed that the theoretical study of composite photovoltaic solar energy converters, given in the First Semiannual Report, should be somewhat extended and refined, and should include calculations based upon the known parameters of silicon and aluminum antimonide. It was further agreed that the final report on subject contract should include a complete bibliography, with particular reference to composite or stacked solar cells and the compound semiconductors AlSb and CdSe. It was pointed out by Mr. Cherry that state-of-the-art samples of composite cells, aluminum antimonide, and dichroic mirrors should be delivered to USASRDL as soon as practicable.

On 22 June 1960 the Project Supervisor visited Drs. F. J. Reid, W. P. Allred, and Mr. W. L. Mefferd at the Battelle Memorial Institute, Columbus, Ohio, to discuss the growth and characterization of AlSb. This visit proved fruitful in that information applicable to the growth of single crystals of this compound was gained.

4. FACTUAL DATA

4.1 A Theoretical Study of the Composite Photovoltaic Solar Energy Converter

4.1.1 Introduction

It is appropriate to divide the analysis of a two-semiconductor composite solar cell into two parts, viz: a theoretical determination of the two semiconducting materials the use of which will result in maximum efficiency, and secondly a study of the effect on efficiency of cell design parameters such as junction depth, to determine the optimum values of these parameters.

Selection of the optimum semiconducting materials for a composite cell requires consideration of the ability of various semiconductors to absorb energy from the solar spectrum, and also of their ability to deliver the absorbed energy to an external load as useful electrical power.

The technology of various semiconductors varies greatly in degree of advancement, and in the subsequent analysis it is assumed that the degree of purity and perfection of structure can ultimately be made equal for all semiconductor materials. (This assumption is made to provide a working basis for analysis, and its validity remains to be determined). Numerical values of the various optical and electronic properties of many semiconductors are not known to a degree of accuracy sufficient to warrant their use; however, the energy gap, one of the most important semiconductor properties, can be taken as a continuously varying function in these analyses, and the solar energy conversion efficiency can be determined as a function of this parameter. This has been done for the case of solar cells employing only one semiconducting element,[1-5] and these results are extended below to the case of composite cells. It should be mentioned in passing that in one aspect the results of Ref. 4 and Ref. 5 are not in agreement; these

discrepancies are discussed in Sections 4.1.3.1 and 4.1.3.2 of this report.

In Section 4.1.2, the spectral efficiency of a composite solar cell is considered. The spectral efficiency is a measure of the ability of the cell to absorb energy from the solar spectrum. Since a semiconductor can absorb energy only from photons of energy greater than its energy gap, and since the maximum energy given to each carrier pair is equal to the energy gap, it is apparent that the spectral efficiency can be determined on the basis of the energy gap alone. In this section the two band gaps are derived which enable a maximum fraction of the solar energy to be absorbed. In general, however, these two band gaps will not be optimum in terms of maximizing power output. From this latter standpoint it is necessary to consider the ability of the semiconductors to deliver the absorbed energy to an external electrical circuit.

In Section 4.1.3 it is shown that the power which a semiconductor can transfer to an external load is strongly affected by a parameter commonly called the reverse saturation current. (This current is known to saturate under reverse bias in germanium p-n junctions, but saturation has not been observed in junctions made from other semiconductor materials). When the reverse current is large, the open-circuit voltage and maximum power output are reduced, and since the reverse current decreases as the energy gap of the semiconductor increases, it is to be expected that materials of higher energy gaps will transfer a larger fraction of absorbed energy to an external load than will materials of lower energy gaps. As a result, one may anticipate that consideration of this parameter will shift the optimum energy gaps to values higher than those determined on the basis of spectral efficiency alone.

The effect on the optimum energy gaps of recombination currents resulting only from radiative recombinations is considered in Section 4.1.3.1. In Section 4.1.3.2 an extension is made to include the case of non-radiative recombinations. The radiative recombinations of electron-hole pairs are unavoidable free-free transitions across the forbidden gap, whereas the non-radiative recombinations of carrier pairs

may, in practice, be reduced. It is shown in Section 4.1.3.2 that the non-radiative recombinations can severely limit the efficiency of a solar cell.

After the optimum energy gaps for a composite cell are determined, it is necessary to consider the effects of cell design parameters on the maximum power output. Two of the most important design parameters in a single cell are the depth of the p-n junction below the cell surface, and the resistivity of the semiconductor. As is well known, the junction depth involves a compromise in that (a), the junction should be very close to the surface so that the maximum number of photon-excited carriers can be collected, and (b), the junction should be deep in order that the resistance of the surface layer, which appears in series with the load resistance, will be a minimum. (This latter consideration can be minimized by gridded contact techniques).

In Section 4.1.4 a simple mathematical model of the cell permits the determination of an approximate expression for the junction current as a function of cell parameters. An expression is derived for the maximum power from a cell considering both the internal diode effect and the series resistance presented by the diffused layer, and the optimum junction depth is derived on the basis of these analyses. Edge leakage currents are not considered in this analysis, since these can be made very small by proper treatment of the cell during fabrication, and since they can be assumed nearly equal for all materials.

The conventional arrangement of the individual elements in a composite solar cell is the stacked or layered configuration in which the cell of higher energy gap is placed immediately above the cell of lower energy gap. The difficulty in this arrangement lies in the insufficient transparency of the higher energy gap cell to photons of energy less than its own excitation energy. Measurements made on intermetallic semiconductors show no better than 75 to 80 percent transmission in this transmission region, and usually much less.[6-9] To be effective, the stacked configuration would require at least 75 percent transmission of the lower energy photons

through the high energy gap element. It is possible that improvements in technology may lead to the required transparency, but a more promising configuration at this time is that in which the two components of the composite cell are situated at 90° to each other, with a dichroic mirror inserted between the components at a 45° angle to each. Such dichroic mirrors are readily available, and can be designed to separate the incident light beam at the optimum wavelength, transmitting the appropriate band of the solar spectrum to the cell of lower energy gap, and reflecting the higher energy photons to the cell of higher band gap. The separation of the spectrum with such mirrors is quite abrupt, as will be shown, and both the long wavelength transmission and short wavelength reflection are between 90 and 95 percent.

It is evident that an investigation of the reflective type cell will prove worthwhile in that it will serve to demonstrate the feasibility of composite cells. Since the dichroic mirror characteristics are superior to what may be expected in the transmission of an intermetallic compound, it follows that failure of the reflective type cell to surpass a single solar cell would insure the failure of the more practical stacked configuration. However, if the reflective composite cell should prove sufficiently superior to a single cell, then further efforts to improve the transmission characteristics of high energy gap materials will be warranted.

4.1.2 The Optimum Energy Gaps for a Composite Solar Cell on the Basis of Spectral Efficiency

The spectral efficiency of a solar cell may be defined as the ratio of the rate of absorption of solar energy as excited electron-hole pairs to the total incident spectral power. Let a composite cell be composed of two semiconductors of band gaps E_{g_1} and E_{g_2}, and let E_{g_2} be greater than E_{g_1}. It is assumed that the incident solar spectrum is divided into two parts by a dichroic mirror, such that all radiation of $h\nu > E_{g_2}$ is

reflected to and absorbed by the cell of energy gap E_{g_2}, and all radiation of $h\nu < E_{g_2}$ is transmitted to the cell of energy gap E_{g_1}. The latter can absorb only those photons for which $h\nu > E_{g_1}$. The arrangement is as shown in Fig. 1.

In this analysis it will be assumed that there are no reflection losses from the cell surfaces, since the optimum energy gaps will not be strongly affected by such losses. Reflection can be reduced to 10 percent or less by the use of suitable cell coatings, and the losses will then be approximately the same for all materials in the range of E_g of interest. It is also assumed that all photons of $h\nu > E_g$ are absorbed.

In general, an electron-hole pair excited in a semiconductor of band gap E_g by a quantum of energy $h\nu$, where $h\nu$ is greater than E_g, absorbs from the quantum a maximum energy E_g. If $N(\lambda)$ is the number of quanta per unit wavelength per unit time in the wavelength increment $d\lambda$, the integrated power absorbed by the semiconductor may be found by summing the number of quanta of energy greater than E_g per unit time, and multiplying by E_g. In the case of the composite solar cell it is necessary to sum those quanta of energy greater than E_{g_2} and multiply the result by E_{g_2}, and also to sum those quanta for which $E_{g_1} < h\nu < E_{g_2}$, and multiply by E_{g_1}. The first operation gives the total power absorbed in the higher-energy-gap cell and the second gives the power absorbed in the lower-energy-gap cell; the sum is simply the absorption by the composite cell. In terms of energy, the total power may be written

$$P = E_{g_2} \int_{E_{g_2}}^{\infty} N(E)dE + E_{g_1} \int_{E_{g_1}}^{E_{g_2}} N(E)dE, \qquad (4\text{-}1)$$

where N(E) is the number of photons per unit time in the energy increment dE around E.

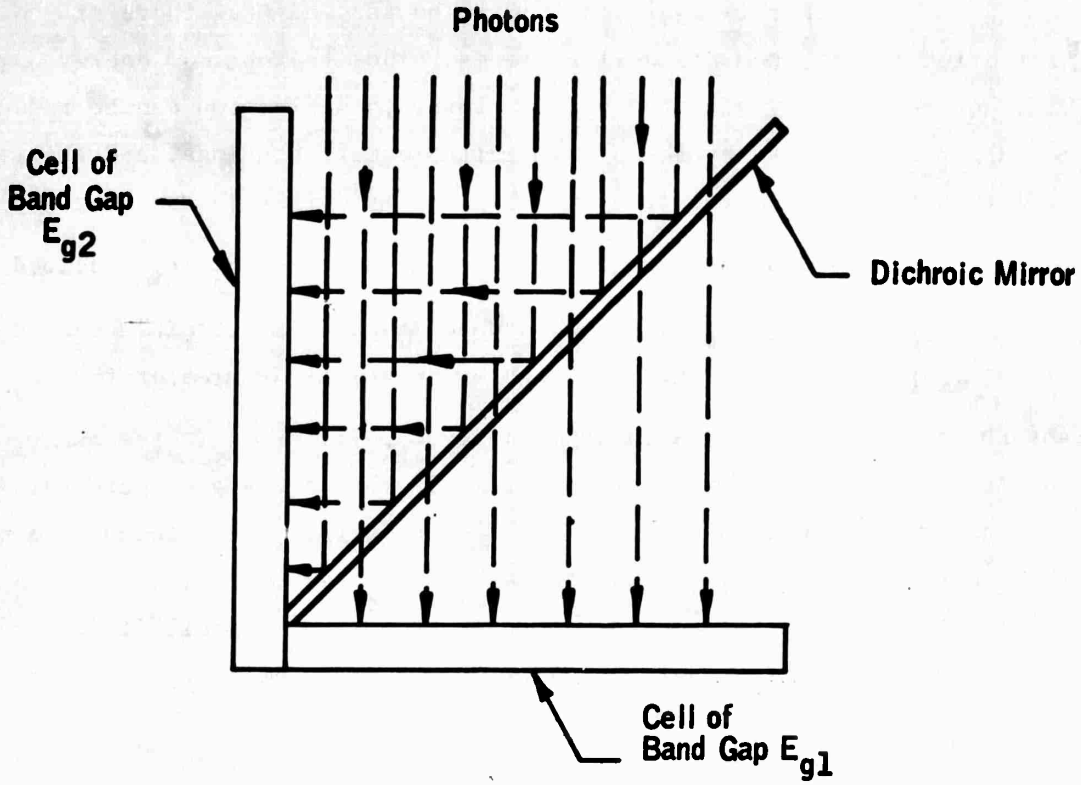

FIG. 1. REFLECTION - TYPE COMPOSITE CELL.

It is obvious that the result obtained from Eq. (4-1) will depend on the solar spectral distribution, since this determines N(E). The problem of preferential atmospheric absorption has been treated in detail by Loferski,[4] and in the present work the only case to be considered is that of air mass zero, corresponding to the spectral distribution beyond the Earth's atmosphere. The spectral distribution given by Johnson[10] will be adopted, and from this distribution, shown in Fig. 2, and using the relation $\nu = E_{ph}/h$ it is possible to compute the number of photons per second of energy greater than E_g as a function of E_g. The result is given in Fig. 3. The y-axis intercept is simply the total number of solar photons, and it may be observed that essentially all of these have $h\nu > 0.4$ eV.

Since the number of photons of energy greater than E_g decreases as E_g increases, it is clear from Eq. (4-1) that there will be an optimum pair of energy gaps which will maximize the absorbed power. If a suitable approximation to the curve of Fig. 3 can be found, then the optimum energy gaps can be determined analytically by carrying out the integrations in Eq. (4-1), simplifying and differentiating the result. This is most easily understood by considering the slope of the curve of Fig. 3. We have

$$N_{ph}(E_g) = \int_0^\infty N(E)dE - \int_0^{E_g} N(E)dE \qquad (4\text{-}2)$$

where $N_{ph}(E_g)$ is the ordinate of Fig. 3, the first integral on the right is the total number of solar photons, and the second integral is the number of photons of energy less than E_g. Differentiating Eq. (4-2):

$$\frac{dN_{ph}(E_g)}{dE} = -N(E_g). \qquad (4\text{-}3)$$

The first integral on the right side of Eq. (4-2) vanishes on differentiation, since the total number of solar photons is constant. The slope

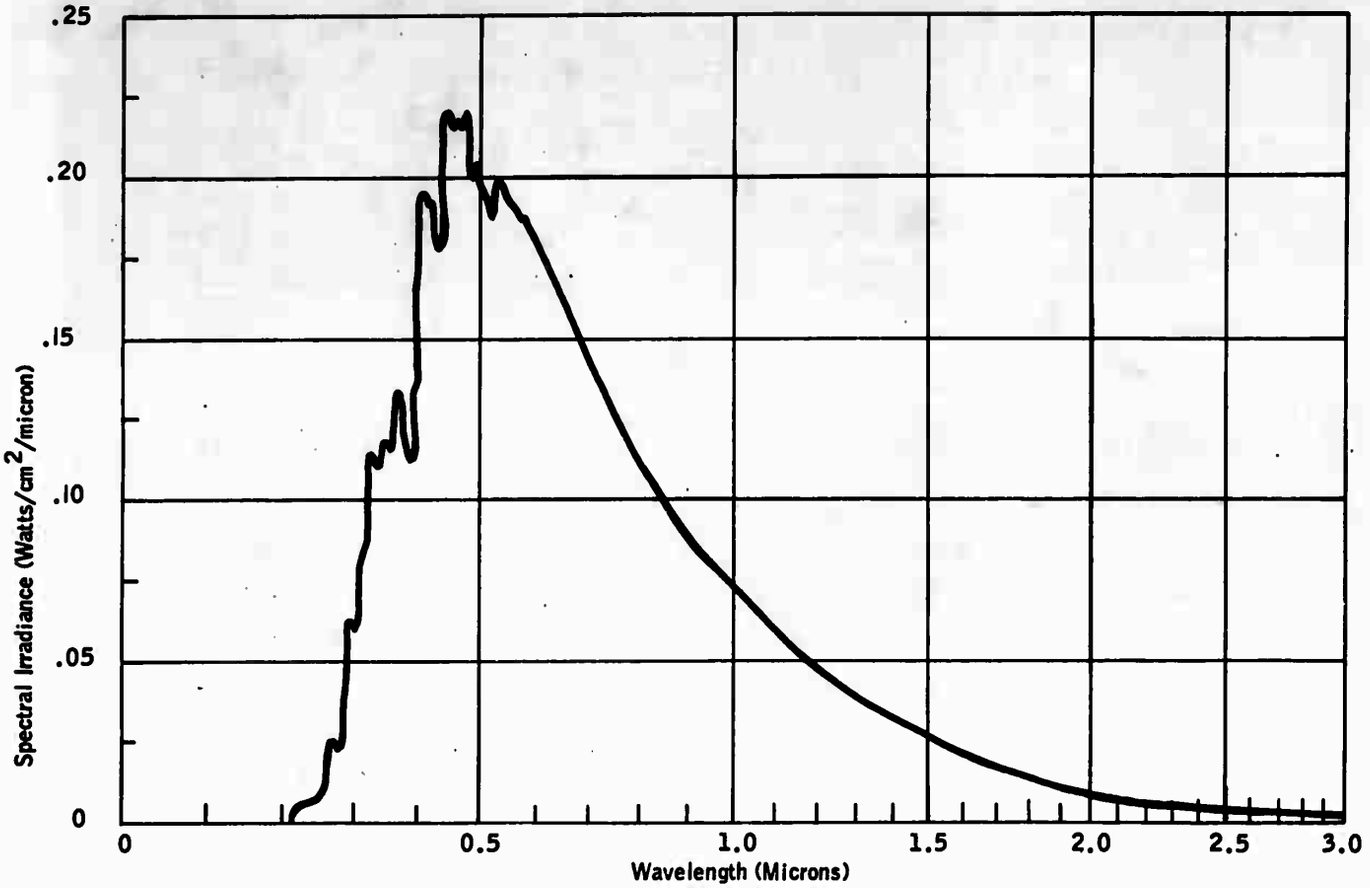

FIG. 2. SOLAR SPECTRAL IRRADIANCE OUTSIDE EARTH'S ATMOSPHERE, CORRECTED TO MEAN SOLAR DISTANCE. (AFTER JOHNSON)

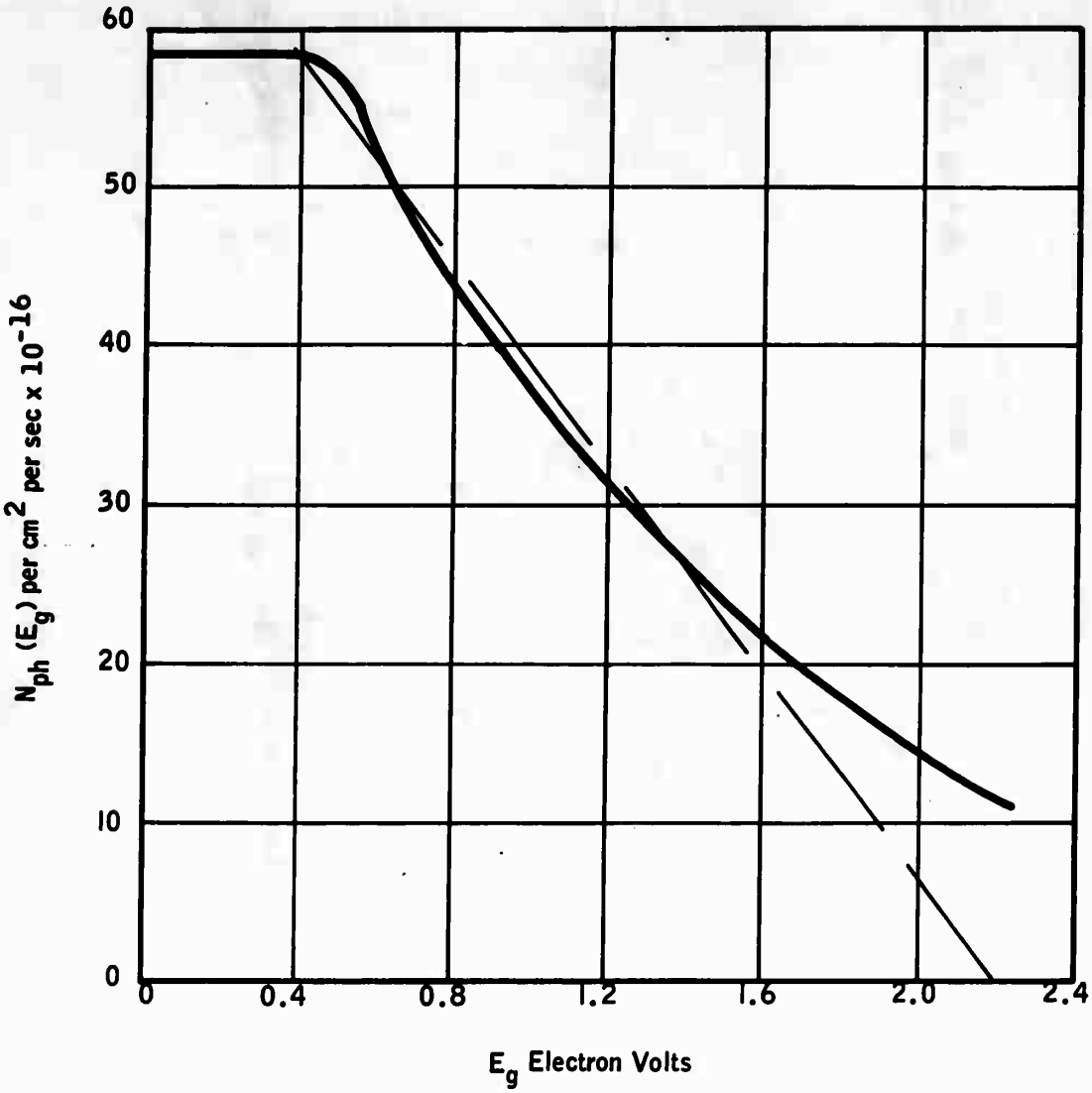

FIG. 3 NUMBER OF PHOTONS/CM^2/SEC OF ENERGY GREATER THAN E_g.

of Fig. 3, then, is seen to be the negative of $N(E_g)$, the number of photons in a range dE around E_g, per unit time, per unit area.

An expression for $N(E_g)$, or $N(E)$, is required in Eq. (4-1), and an approximate numerical value can be obtained by approximating the curve of Fig. 3 by two straight line segments, one of zero slope and ordinate 58×10^{16} from 0.0 to 0.4 eV, and the other from coordinates $(0.4, 58 \times 10^{16})$ to (2.2, 0.0). This gives a negative slope of magnitude $\frac{58}{1.8} \times 10^{16}$ units. Thus,

$$N(E_g) \begin{cases} = 0 \text{ for } E_g < 0.4 \text{ eV} \\ = \frac{58}{1.8} \times 10^{16} \text{ for } 0.4 < E_g < 2.2 \text{ eV} \\ = 0 \text{ for } E_g > 2.2 \text{ eV}. \end{cases}$$

Rewriting Eq. (4-1) for convenience

$$P = E_{g_2} \int_{E_{g_2}}^{\infty} N(E_g)dE + E_{g_1} \int_{E_{g_1}}^{E_{g_2}} N(E_g)dE$$

and using the constant values of $N(E_g)$ given above, we have for the power absorbed,

$$P = E_{g_2} \int_{E_{g_2}}^{2.2} \left(\frac{58}{1.8} \times 10^{16}\right)dE + E_{g_1} \int_{E_{g_1}}^{E_{g_2}} \left(\frac{58}{1.8} \times 10^{16}\right)dE$$

$$= \frac{58}{1.8} \times 10^{16} \left[E_{g_2}(2.2 - E_{g_2}) + E_{g_1}(E_{g_2} - E_{g_1})\right]$$

$$= \frac{58}{1.8} \times 10^{16} \left[2.2\,E_{g_2} - E_{g_2}^2 + E_{g_1}E_{g_2} - E_{g_1}^2\right] . \qquad (4\text{-}4)$$

For a maximum value,

$$\left.\begin{aligned} \frac{\partial P}{\partial E_{g_1}} &= 0 = E_{g_2} - 2E_{g_1} \\ \frac{\partial P}{\partial E_{g_2}} &= 0 = 2.2 - 2E_{g_2} + E_{g_1} . \end{aligned}\right\} \qquad (4\text{-}5)$$

The solutions of Eqs. (4-5) are

$$E_{g_1} = 0.73 \text{ eV}, \quad E_{g_2} = 1.46 \text{ eV}.$$

These are the values of the energy gaps in the composite solar cell resulting in maximum power absorption from the solar spectrum, and therefore maximum spectral efficiency.

It must be remembered, of course, that these results are based on the spectral efficiency alone. They are modified in the subsequent sections by considering the effect of recombination currents. Before proceeding, it should be pointed out that the approximation used in the foregoing analysis, namely that of approximating the curve of Fig. 3 by a straight line, has been justified by additional calculations wherein the curved portion from 0.4 to 2.2 eV was more closely approximated. The results were not significantly different from those given above with the simpler approximation.

4.1.3 The Optimum Energy Gaps and Maximum Efficiency as Affected by Recombination Currents

A determination of the optimum energy gaps for a composite cell involves consideration of both the expected spectral efficiency as given above, and of the ability of the semiconductors to convert the absorbed solar energy into useful electrical energy. It will be assumed that the fraction of excited electron-hole pairs which reach the junction in a solar

cell is not a function of the band gap. An important parameter which is dependent on the band gap is the reverse saturation current I_o. The irradiated p-n junction may be regarded as a constant current generator in parallel with a non-linear impedance, the characteristic of the latter being approximated by the ideal rectifier equation

$$I = I_o \, (\exp(qV/kT)-1), \qquad (4\text{-}6)$$

where I_o is the reverse saturation current, q is the electronic charge, k is Boltzmann's constant, T is the absolute temperature, and I and V are the current and voltage, respectively.[11-13] The quantity kT/q may be regarded as a thermal generation voltage. Eq. (4-6) is valid only when non-radiative recombinations are absent. The modification to include non-radiative recombinations is given in Section 4.1.3.2. When a load is connected to a solar cell, the load current is simply that produced by the constant current generator less the fraction shunted through the non-linear impedance. This latter fraction of current, I_o (exp(qV/kT)-1), is a forward diode current in an irradiated solar cell. Thus,

$$I = I_L - I_o \, (\exp(qV/kT)-1), \qquad (4\text{-}7)$$

where I_L is the total current produced by photon excitation, V is the junction voltage, and I is the load current. We shall use this equation as the starting point for the analysis of the effect of the recombination currents on the optimum energy gaps and on the conversion efficiency. Eq. (4-6) and (4-7) are derived from generation and recombination rates in Section 4.1.3.2.

In the next section the dependence of I_o on the energy gap will be considered, and calculations of efficiency as a function of E_g will be presented. In the following section evidence will be given to indicate that the recombination currents as expressed in Eq. (4-7) are the result of radiative recombinations only, and that consideration of

non-radiative recombinations results in much lower values for the efficiency and a shift in the optimum energy gaps toward higher values.

4.1.3.1 Diode Currents Resulting Only From Radiative Recombinations

We begin with Eq.(4-7) and assume, for the present, that the diode current shunted through the internal impedance results from radiative recombinations.

$$I = I_L - I_o \left(\exp(qV/kT)-1\right). \tag{4-7}$$

In the range of V of interest, namely near maximum power, $\exp(qV/kT) \gg 1$, therefore we may write

$$I = I_L - I_o \exp\left(qV/kT\right). \tag{4-8}$$

The power delivered to the load is

$$P = IV = V\left[I_L - I_o \exp\left(qV/kT\right)\right] \tag{4-9}$$

For maximum power,

$$d(IV) = IdV + VdI = 0 \tag{4-10}$$

or

$$\frac{dI}{dV} = -\frac{I}{V}. \tag{4-11}$$

But from Eq. (4-8)

$$\frac{dI}{dV} = -\frac{qI_o}{kT} \exp\left(qV/kT\right). \tag{4-12}$$

Equating the right hand sides of Eqs. (4-11) and (4-12), and using the value of I from Eq. (4-8), we have

$$\frac{qV}{kT} \exp (qV/kT) = \frac{I_L}{I_o} - \exp (qV/kT) \qquad (4\text{-}13)$$

or

$$(1 + qV/kT) \exp (qV/kT) \simeq \frac{qV}{kT} \exp (qV/kT) \simeq \frac{I_L}{I_o} . \qquad (4\text{-}14)$$

Then

$$\frac{qV}{kT} = \ln \frac{I_L}{I_o} - \ln \frac{qV}{kT} \qquad (4\text{-}15)$$

As a first approximation, let $\frac{qV}{kT} = \ln \frac{I_L}{I_o}$ and insert into Eq. (4-15) to get

$$\frac{qV}{kT} \simeq \ln \frac{I_L}{I_o} - \ln\ln \frac{I_L}{I_o} . \qquad (4\text{-}16)$$

With the aid of Eq. (4-16) the load current can now be written as

$$I = I_L - I_o \exp (qV/kT) = I_L - \frac{I_L}{\ln (I_L/I_o)}$$

$$= I_L \left[1 - \frac{1}{\ln (I_L/I_o)} \right] . \qquad (4\text{-}17)$$

Now the power, P, is equal to IV, and using Eq. (4-17) for I and the approximations of Eqs. (4-15) and (4-16) for V, the power may be written as

$$P = IV = \frac{kT}{q} I_L \ln \frac{I_L}{I_o} \left[1 - \frac{1}{\ln (I_L/I_o)} \right]$$

$$= \frac{kT}{q} I_L \left[\ln \frac{I_L}{I_o} - 1 \right] \simeq \frac{kT}{q} I_L \ln \frac{I_L}{I_o} . \qquad (4\text{-}18)$$

The result of the foregoing approximations is simply the product of the open-circuit-voltage and short-circuit-current of the device, and as such is not sufficiently accurate for numerical calculations of the efficiency. However, Eq. (4-18) serves to illustrate the strong dependence of the power output of the device, and hence the efficiency, on the reverse saturation current I_o.

A relationship relating the reverse saturation current to the intrinsic carrier concentration, and therefore E_g, has been derived by Shockley,[14] and may be written as

$$I_o = kTq\mu_n\mu_p \left[\frac{1}{\sigma_n L_p} + \frac{1}{\sigma_p L_n}\right] n_i^2 \qquad (4\text{-}19)$$

where

n_i = intrinsic carrier concentration

σ_n = conductivity of n-type material

σ_p = conductivity of p-type material

L_n = diffusion length for electrons in p-region

L_p = diffusion length for holes in n-region

μ_n = electron mobility

μ_p = hole mobility

q = magnitude of electronic charge

and kT has the usual meaning. Eq. (4-19) may be put in several different forms by introducing the mobility ratio

$$b = \mu_n/\mu_p$$

and making use of the fact that the intrinsic conductivity σ_i, is given by

$$\sigma_i = q\mu_p n_i(1 + b).$$

Thus, in terms of the intrinsic conductivity,

$$I_o = \frac{kT}{q} \cdot \frac{b}{(1+b)^2} \left[\frac{1}{\sigma_n L_p} + \frac{1}{\sigma_p L_n} \right] \sigma_i^2 \qquad (4\text{-}20)$$

The dependence of the optimum energy gaps on I_o can now be introduced, since the square of the intrinsic carrier concentration, which appears in Eq. (4-19) has been shown[15] to be

$$n_i^2 = 4 \left(\frac{2\pi kT}{h^2} \right)^3 (m_n m_p)^{3/2} e^{-E_g/kT} \qquad (4\text{-}21)$$

where h = Planck's constant, and m_n and m_p are the electron and hole effective masses, respectively. Thus, Eq. (4-19) may be written

$$I_o = kTq\mu_n\mu_p \left(\frac{1}{\sigma_n L_p} + \frac{1}{\sigma_p L_n} \right) \left[4 \left(\frac{2\pi kT}{h^2} \right)^3 (m_n m_p)^{3/2} \right] e^{-E_g/kT} \qquad (4\text{-}22)$$

This expression may be used to compute I_o for various semiconducting materials, but since the values of the various parameters are not known for all materials, and since we are concerned primarily with the dependence on the energy gap, we shall assume, perhaps unrealistically, that except for E_g, the parameters can be taken as equal for all materials.

With this assumption, the actual numerical work can be simplified by again making use of Eq. (4-21). We may write Eq. (4-22) as

$$I_o = \left\{ kTq\mu_n\mu_p \left[\frac{1}{\sigma_n L_p} + \frac{1}{\sigma_p L_n} \right] \frac{n_i^2}{e^{-E_g/kT}} \right\}_{\text{silicon}} e^{-E_g/kT} \qquad (4\text{-}23)$$

where, for the purpose of numerical calculations, all parameters enclosed within the brackets are taken to be those of silicon. Such calculations have been made for a single cell by Loferski,[4] who made use of the fact that in a given material at a given temperature, the product of the

electron and hole concentrations is equal to the square of the intrinsic concentration, and also the fact that

$$\sigma_i = n_i q (\mu_n + \mu_p)$$

to write* Eq. (4-20) as

$$I_o = \frac{kT}{q} \cdot \frac{b}{(1+b)^2} \left[\frac{1}{\sigma_n L_p} + \frac{1}{\sigma_p L_n}\right] \sigma_i \quad \left(n_i q (\mu_n + \mu_p)\right)$$

$$= \frac{b}{(1+b)^2} \; kT \; (\mu_n + \mu_p) \left[\frac{1}{\sigma_n L_p} + \frac{1}{\sigma_p L_n}\right] (N_p N_n)^{1/2} \sigma_i \, . \qquad (4\text{-}24)$$

A factor $\exp(-E_g/2kT)$ can be taken out of each of $(N_p N_n)^{1/2}$ and σ_i to arrive at the same exponential dependence of I_o on E_g as in Eq. (4-23) above. We shall write the saturation current given in Eq. (4-23) as

$$I_o = A\exp(-E_g/kT) \qquad (4\text{-}25)$$

Numerical calculations based on this dependence of I_o have been carried out in the manner described in Ref. 4, but for the case of a composite cell arranged as in Fig. 1. The value of the coefficient A in Eq. (4-25) was computed to be 0.825×10^8 amperes/cm^2. In calculating the light-generated current, I_L (see Eq. (4-7) the incident photon density on each cell was reduced by five percent from the value it would have if the dichroic mirror introduced no losses, i.e., it was assumed that the dichroic separates the incident beam in an abrupt step fashion, but has 95 percent transmission at the longer wavelengths and 95 percent reflection at the shorter wavelengths. This permits a reasonable comparison of the resulting efficiency with the data in the literature pertaining to single

---

* Note that as a result of a printer's error the factor σ_i in Eq. (4-24) has been omitted in Eqs. (9) and (10) of Ref. 4.

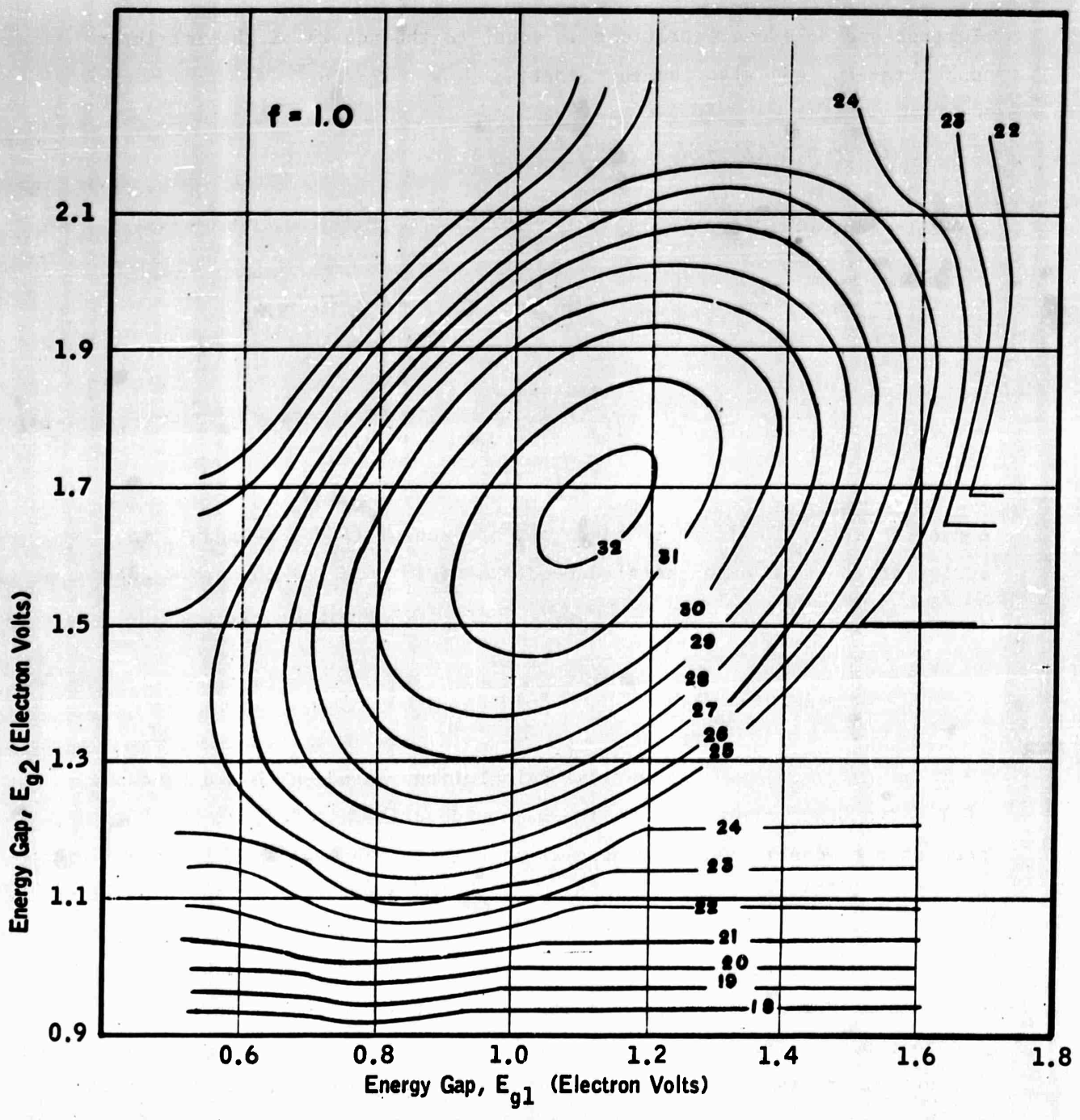

FIG. 4. EFFICIENCY CONTOURS FOR COMPOSITE CELL AS A FUNCTION OF ENERGY GAPS; NO NON-RADIATIVE RECOMBINATION. $I_o = A \exp(-E_g/kT)$. Percent efficiency is given on each curve.

cells. It was also taken that the separation of the incident beam by the dichroic occurs at the wavelength corresponding to E_{g_2}, so that all radiation of $h\nu > E_{g_2}$ is reflected to the cell of band gap E_{g_2}.

Reflection losses at the surfaces of the two cells were neglected, since these are not expected to affect the position of the optimum energy gaps. To simplify the calculations, the assumption of Section 4.1.2, namely that the curve of Fig. 3 could be approximated by two straight lines, was retained. The air mass was taken to be zero, and the incident solar power 135 mw/cm^2.

The results for this case are plotted in Fig. 4. The ordinate is the energy gap of the higher gap cell, E_{g_2}, and the abcissa is the energy gap of the lower gap cell, E_{g_1}. Curves of constant efficiency are plotted, the numerical value of the efficiency being given on each curve so that the result may be regarded as a "contour map." The linear approximation to Fig. 3 causes the curves to be nearly symmetrical ellipses.

It is seen that the maximum efficiency occurs for $E_{g_1} = 1.12$ eV and $E_{g_2} = 1.67$ eV, which should be compared with the values of 0.73 eV and 1.46 eV obtained in Section 4.1.2 before considering recombination currents. The optimum values are higher as expected. The maximum theoretical efficiency in this case is about 32.5 percent. It was found that the maximum theoretical efficiency of a single cell, based on the same calculations, is 24.4 percent at about 1.4 eV; thus a significant potential efficiency gain is indicated for the composite cell.

The consideration that all photons of $h\nu > E_{g_2}$ should be directed to the cell of band gap E_{g_2} causes the contours of Fig. 4 to open up in the region where $E_{g_1} > E_{g_2}$. In this region the cell of

band gap E_{g_1} receives no energy which it can absorb, so that the efficiency contours become straight horizontal lines at the value of E_{g_2} for which a single cell of band gap E_{g_2} will give the particular value of efficiency. The efficiency contours are closed curves only when the efficiency exceeds that obtainable in a single cell. For low values of E_{g_1}, the contribution by the cell of band gap E_{g_1} decreases with E_{g_1}, and the contours again approach straight lines at the value of E_{g_2} for which a single cell of band gap E_{g_2} will give the particular value of efficiency. If the efficiencies were computed for sufficiently high values of E_{g_2}, such that the contribution from the high energy gap cell became very small and the dichroic mirror did not cut off radiation from the low-energy-gap cell, the contours at the top of the map would approach straight vertical lines at the value of E_{g_1} for which a single cell of band gap E_{g_1} would give the particular value of efficiency.

In addition to the optimum energy gaps, the curves give information in regard to the pairing of materials, in that the optimum E_{g_2} for any value of E_{g_1} can be read from Fig. 4.

We shall defer the discussion of non-radiative recombinations until Section 4.1.3.2, and consider now the possibility of the dependence of I_o on E_g being of the form

$$I_o = \exp(-E_g/nkT) \qquad (4\text{-}26)$$

where n is greater than one. A dependence of I_o on E_g as in Eq. (4-26)

was assumed by Loferski[4] (1956), on the basis of the results of other authors.[16, 17] In particular, it had been shown that the reverse current in silicon p-n junctions did not saturate as would be expected from the ideal rectifier equation, and furthermore the forward current in germanium had been found by Hall to vary more slowly than exp(qV/kT). More recent work[18,5] has served considerably to clarify the nature of the forward and reverse currents. This is discussed in the section following, and leads to results differing from those obtained on the basis of Eq. (4-26). Nevertheless, for the purpose of a comparison with the earlier results for a single solar cell, it is felt worthwhile to include the calculations for a composite solar cell based on the I_o dependence given in Eq. (4-26).

The composite cell efficiency has been computed for this case with n = 2, and the results are shown in Fig. 5. The calculations are again for air mass zero, and are the same as those for Fig. 4 in all respects except for I_o.

There are three points to notice in comparing Fig. 5 with Fig. 4. Firstly, the optimum energy gaps have been lowered from E_{g_1} = 1.12 eV and E_{g_2} = 1.67 eV to E_{g_1} = 0.8 eV and E_{g_2} = 1.5 eV. Secondly, the maximum efficiency has dropped from 32.5 percent to about 24.7 percent, and lastly the fall off in efficiency is much less steep in Fig. 5 than in Fig. 4, indicating that the choice of the optimum energy gaps is not as critical if $I_o = \exp(-E_g/2kT)$. The latter point appears as a wider separation between contour lines in Fig. 5, the contours being shown for unit steps of efficiency in both cases. The maximum efficiency of a single cell for the case where $I_o = \exp(-E_g/2kT)$ was found to be 19.1 percent at E_g = 1.17 eV, compared with the 24.7 percent obtained with the composite cell. It should be noticed further that in the region of low energy gaps the efficiency is higher in the case where $I_o = \exp(-E_g/2kT)$ than in that where $I_o = A\exp(-E_g/kT)$. This model may be the least satisfactory of those considered and other approaches are given below.

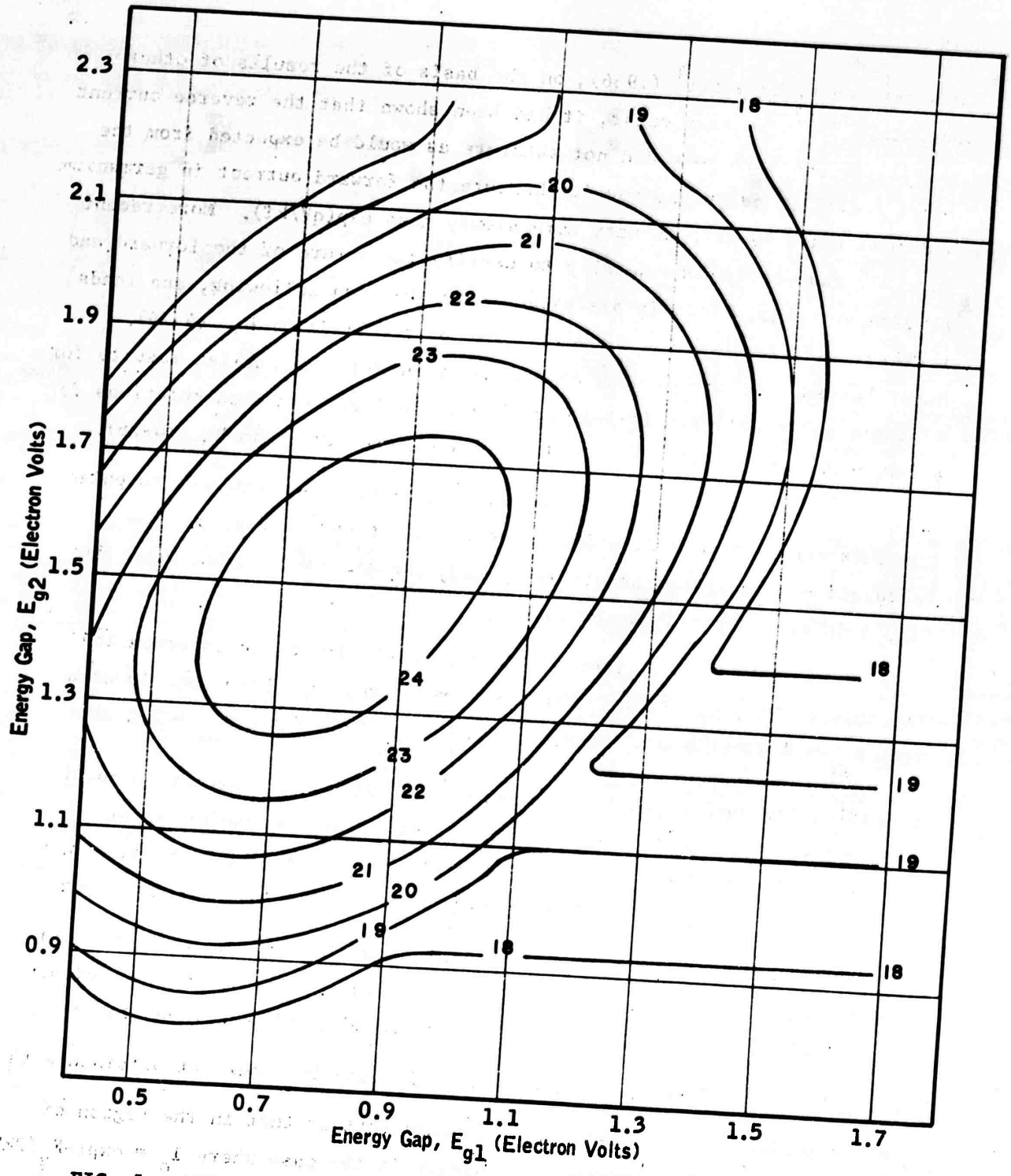

FIG. 5. EFFICIENCY CONTOURS FOR COMPOSITE CELL AS A FUNCTION OF ENERGY GAPS. $I_o = \exp(-E_g/2kT)$

4.1.3.2 Diode Currents Resulting from both Radiative and Non-Radiative Recombinations

The introduction of the factor n into the exponent in Eq. (4-26) requires that the Shockley predicted coefficient in Eqs. (4-22) and (4-23) be arbitrarily set equal to 1.0 amperes/cm^2, rather than approximately 10^8 amperes/cm^2. This follows from the fact that in silicon, for example, $\exp(-E_g/kT) \simeq 10^{-20}$ at room temperature, whereas $\exp(-E_g/2kT) \simeq 10^{-10}$. If the value of 10^8 amp/cm^2 were used for the coefficient in the latter case, the cell efficiency would vanish. From an empirical viewpoint this is satisfactory if it results in a closer fit to the experimentally observed facts. However, the more recent work by Sah, et. al.,[18] permits a more definitive analysis; namely, it was shown that in the case of a p-n junction biased in the reverse direction there is for bias of several kT/q, a component of current flowing in the external circuit given by

$$I_D = -I_o = -A\exp(-E_g/kT) \qquad (4\text{-}27)$$

which is, except for the sign, identical with Eqs. (4-23) and (4-25). Further, there is a second current component given by

$$I_G = \frac{-qWn_i}{2\tau_o} \quad \text{amps/cm}^2 \qquad (4\text{-}28)$$

where q = electronic charge

W = transition layer width

n_i = intrinsic carrier concentration

τ_o = minority carrier lifetime,

and I_G is a current density, the area of the junction being omitted from the right hand side. The current given in Eq. (4-28) results from the fact that in a reversely biased p-n junction both types of charge carriers are swept out of the transition region by the large electric field in that region at an extremely rapid rate. Rapid thermal generation of carriers

in the transition region is necessary to replenish those swept out by the field. For every pair of carriers thus generated, one electron flows in the external circuit, giving rise to the current in Eq. (4-28).

We need not concern ourselves with the conditions of large reverse bias, but it may be pointed out that in this case also the space charge or transition layer width, W, appears in the expression for I_G, the generation current. Failure of the reverse current to saturate under large reverse bias in those materials for which $I_G \gg I_D$ results from the fact that in a reversely-biased linearly-graded junction the space charge layer width increases as the 1/3 power of the applied bias.

We may now briefly review the theory of a p-n junction biased in the forward direction, after which we may proceed to the corresponding analysis of solar cell efficiency. In the forward bias condition, there are again two components of current. For small or medium values of bias (several kT/q) there is the customary diffusion current given by

$$I_D = I_o \exp(qV/kT) \qquad (4\text{-}29)$$

where I_o is given by Eqs. (4-23) or (4-25). For large forward bias, the exponential dependence of I_D becomes exp(qV/2kT). This occurs, however, for biases considerably larger than that for which the recombination current, discussed below, assumes such a dependence. Indeed, in Appendix IV of Ref. 18, it was shown that in 1.0 ohm-cm silicon the lower limit of bias voltage for this case is 0.75 volts, and minimum current density 43 amps/cm^2. In the case of materials doped to a resistivity level suitable for use in solar cells, the minimum value of bias voltage for the exp(qV/2kT) dependence of the diffusion current is still higher, and we need consider only the case where the diffusion current varies as exp(qV/kT).

The second component of current under forward bias is a non-radiative recombination current, being the reverse process of the generation current found in reverse bias. It results from carrier recombination at trapping centers within the space charge layer. This current may have an exponential dependence given by exp(qV/kT) or exp(qV/nkT), depending on the depth of the traps in the forbidden band.[18] If the traps are deep, (at or near the intrinsic Fermi level) the recombination current varies as exp(qV/nkT), where n is greater than one, but slightly less than two. When the traps are shallow (about 10 kT from the intrinsic Fermi level) the recombination current varies as exp(qV/kT).

If the forward bias is several kT/q or less, the recombination current is larger than the diffusion current, and it dominates. The forward current in the case of deep traps and small or medium bias will therefore vary considerably more slowly than exp(qV/kT), the rate approaching exp(qV/2kT), since the total forward current is the sum of the diffusion current I_o exp(qV/kT) and the recombination current $I_R \propto$ exp(qV/nkT). For very shallow traps, the recombination current varies as exp(qV/kT) and, again for small or medium bias, the exponential dependence of the forward current is similarly exp(qV/kT). It should be noted that exp(qV/kT) is the maximum rate of variation of the forward current. In the case of large forward bias, the recombination current is negligible compared to the diffusion current, and the exponential dependence of the forward current depends upon the particular value of bias and the doping level of the material. As mentioned previously this case need not be considered in a discussion of solar cells.

We are now in a position to derive an expression for the load current delivered by a solar cell considering both radiative and non-radiative recombinations. It will be recalled that an insolated solar cell is biased in the forward direction, and we need consider the reverse current I_o, but not the reverse generation current I_G. The former governs the forward diffusion current; the latter is replaced by the forward non-radiative recombination current, I_R.

It was pointed out in Ref. 5 that an analysis of solar cell characteristics should begin by equating the total carrier generation rate to the total removal rate, thus:

$$S + C_n(0) = C_n(V) + C_r(V) + I/q. \qquad (4\text{-}30)$$

Here S = rate of pair generation by incident sunlight,

$C_n(0)$ = non-radiative thermal generation rate, independent of the voltage V,

$C_n(V)$ = non-radiative recombination rate, a function of V,

$C_r(V)$ = radiative recombination rate, a function of V,

I/q = rate of carrier removal to load.

It was further suggested, though not shown explicitly, that the effect of non-radiative recombinations on solar cell performance could be considered by introducing a factor f, where f is the ratio of the radiative recombination rate to the total recombination rate. That this can indeed be done is shown below.

The terms in Eq. (4-30) are converted to current components by multiplying by the charge q. Thus qS is the light-generated current, which we shall denote as I_L. The product $qC_n(0)$ is the non-radiative thermal generation current, commonly called the reverse saturation current, I_o, and given by Eqs. (4-19), (4-20), or (4-25), and $qC_n(V)$ is a non-radiative recombination current, resulting from recombinations in the space charge layer under forward bias as discussed above. The exponential dependence of $qC_n(V)$ on V is a function of the depth of the recombination levels as previously pointed out. The current given by $qC_r(V)$ is a radiative recombination current, and in the discussion of forward biased p-n junctions it was referred to as the diffusion current, I_D; it is given by $I_D = I_o \exp(qV/kT)$ as in Eq. (4-29). We shall hereafter refer to $qC_r(V)$ as the radiative recombination current to distinguish it from that due to non-radiative recombinations. The current I is simply the load current delivered by the solar cell.

There are four cases to consider, as follows:

Case I A Solar Cell in Which There are no Non-Radiative Recombinations

In this case $C_n(V) = 0$, and we have

$$S + C_n(0) = C_r(V) + I/q \tag{4-31}$$

or, on multiplying by q:

$$I_L + I_o = I_o\, e^{qV/kT} + I. \tag{4-32}$$

Solving Eq. (4-32) for the load current, I,

$$I = I_L + I_o - I_o\, e^{qV/kT}$$

$$= I_L - I_o \left(e^{qV/kT} - 1 \right) . \tag{4-33}$$

This is the usual equation given for a solar cell, as Eq. (4-7). It is noted that non-radiative recombinations are not considered.

Case II A Forward Biased p-n Junction with no Non-Radiative Recombinations

In this case $S = 0$, $C_n(V) = 0$, and the "load" current changes sign, since it is now delivered to the junction by a bias battery.

$$C_n(0) = C_r(V) - I/q \tag{4-34}$$

and on multiplying by q,

$$I_o = I_o\, e^{qV/kT} - I$$

or $$I = I_o \left(e^{qV/kT} - 1 \right) . \tag{4-35}$$

This is the ideal rectifier equation, and again non-radiative recombinations are not considered.

The two remaining cases are identical except for the inclusion of the non-radiative term. As discussed previously, the exponential dependence of the non-radiative recombination current under forward bias is a function of the depth of the trap levels, and an explicit term cannot be added to Eqs. (4-33) or (4-35) to account for this. Furthermore since the forward current is a sum of two currents of differing exponential dependence on V, the exponent in the radiative component should not arbitrarily be altered to account for the non-radiative term. Rather, if we let f be the ratio of the radiative recombination rate to the total recombination rate, the non-radiative term can be introduced without disturbing the exponential dependence of the other term. Thus:

$$f = \frac{C_r(V)}{C_r(V) + C_n(V)} \leq 1 \qquad (4\text{-}36)$$

and solving for $C_n(V)$,

$$fC_r(V) + fC_n(V) = C_r(V)$$

$$C_n(V) = \frac{1}{f} C_r(V) - C_r(V). \qquad (4\text{-}37)$$

Using Eq. (4-37) for $C_n(V)$, we may consider Cases III and IV.

Case III A Solar Cell; General Case

Rewriting Eq. (4-30):

$$S + C_n(0) = C_n(V) + C_r(V) + I/q$$

Substituting Eq. (4-37):

$$S + C_n(0) = \frac{1}{f} C_r(V) - C_r(V) + C_r(V) + I/q \qquad (4\text{-}38)$$

Cancelling like terms and multiplying by q,

$$I_L + I_o = \frac{1}{f} I_o e^{qV/kT} + I \qquad (4\text{-}39)$$

Solving for the load current, I,

$$I = I_L - I_o\left(\frac{1}{f} e^{qV/kT} - 1\right) . \qquad (4\text{-}40)$$

Eq. (4-40) is an expression for the general case. It must be understood that V and f are not independent of each other. The factor f explains the low value of open-circuit-voltage found in poor solar cells, as can be seen by setting I = 0 and solving for V_{oc}. Thus, if we assume $\frac{1}{f}$ exp (qV/kT)>>1.0,

$$V_{oc} = \frac{kT}{q} \ln \frac{fI_L}{I_o} \qquad (4\text{-}41)$$

In the ideal case of no non-radiative recombinations, f = 1.0, and V_{oc} is a maximum. Non-radiative recombinations may reduce f to extremely small values and thereby limit the value of V_{oc}.

Case IV A Forward Biased p-n Junction; General Case

As in Case II, S = 0, and I/q changes sign.

$$C_n(0) = C_n(V) + C_r(V) - I/q \qquad (4\text{-}42)$$

Again using Eq. (4-37)

$$C_n(0) = \frac{1}{f} C_r(V) + C_r(V) - C_r(V) - I/q$$

$$I_o = \frac{1}{f} I_o e^{qV/kT} - I \qquad (4\text{-}43)$$

and

$$I = I_o \left(\frac{1}{f} e^{qV/kT} - 1\right) . \qquad (4\text{-}44)$$

Eqs. (4-33), (4-35), (4-40), and (4-44) explain the forward biased p-n junction characteristics satisfactorily. The failure of the reverse current to saturate may be explained by sufficiently

small values of f, but this is better considered through the nature of the generation current under reverse bias, and the space charge layer width.

Eq. (4-40) for the general case of a solar cell may be employed to calculate the cell efficiency as a function of E_g. The procedure for a composite cell is the same as that used in obtaining Fig. 4, except for the introduction of the factor f. The dependence of the reverse current, or non-radiative thermal generation current I_o, is again taken to be $\exp(-E_g/kT)$. Calculations were made for values of f of 10^{-3}, 10^{-6}, and 10^{-9}, the latter being an extreme case. The same p-n junction parameter values were used as in determining Fig. 4. (Fig. 4 represents f = 1.0).

The efficiency contours for f = 10^{-3}, 10^{-6}, and 10^{-9} are given in Figs. 6, 7, and 8, respectively, and the results are summarized in Table I, which includes Fig. 4 with f = 1.0.

T A B L E I.

The Dependence of Cell Efficiency and Optimum Band-Gaps on Recombination Currents.

Fig. No.	f	Max. Eff. Composite Cell	Optimum Gaps		Max. Eff. Single Cell
			E_{g_1}	E_{g_2}	
4	1.0	32.5%	1.12 eV	1.67 eV	24.4% at 1.4 eV
6	10^{-3}	25.5	1.24	1.72	19.4 at 1.45
7	10^{-6}	19.8	1.37	1.78	14.9 at 1.54
8	10^{-9}	14.1	1.48	1.84	10.8 at 1.65

It may be observed that as the fraction of non-radiative recombination increases, causing f to decrease, the

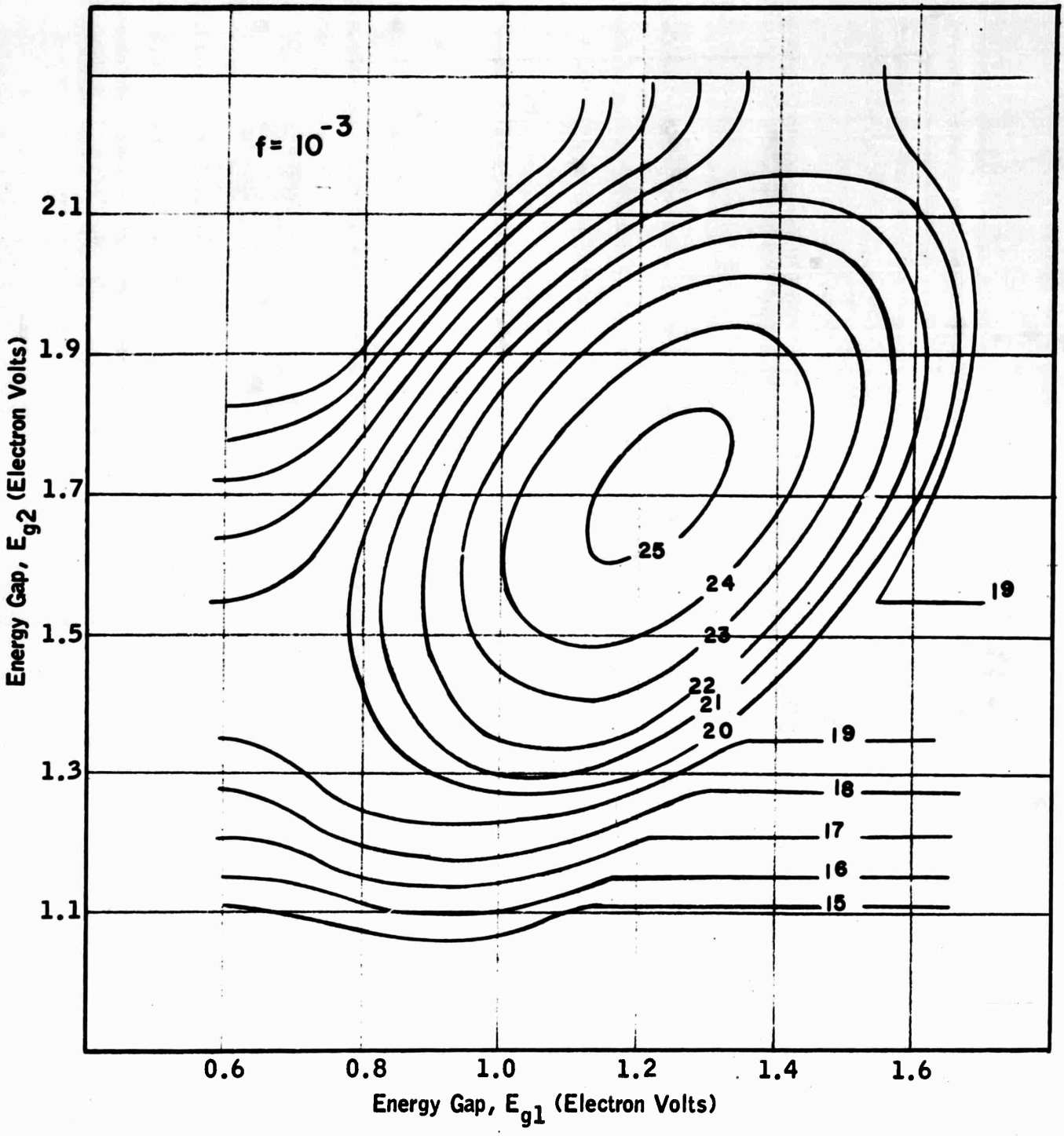

FIG. 6 EFFICIENCY CONTOURS FOR COMPOSITE CELL AS A FUNCTION OF ENERGY GAPS. $f = 10^{-3}$.

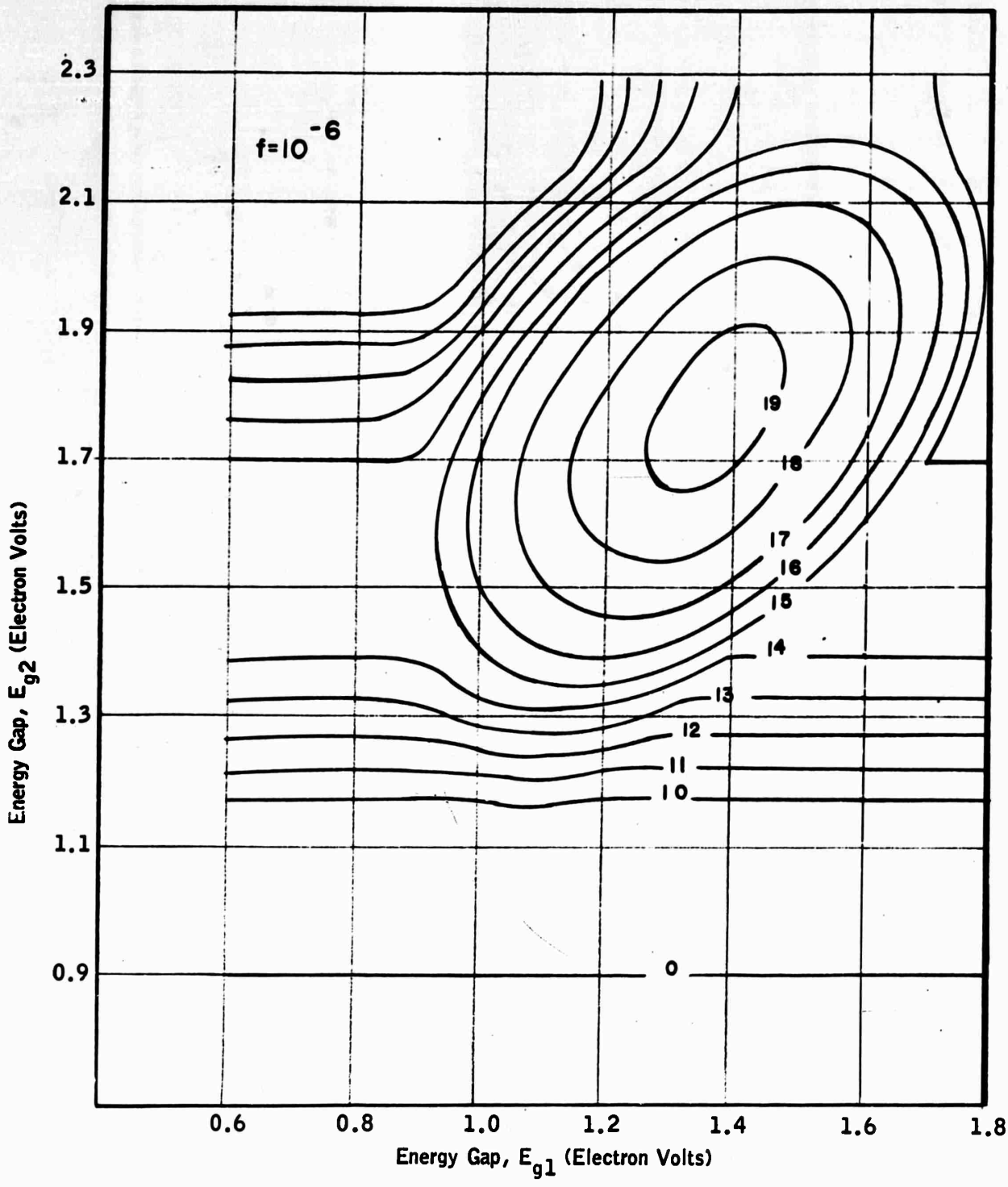

FIG. 7. EFFICIENCY CONTOURS FOR COMPOSITE CELL AS A FUNCTION OF ENERGY GAPS. $f = 10^{-6}$.

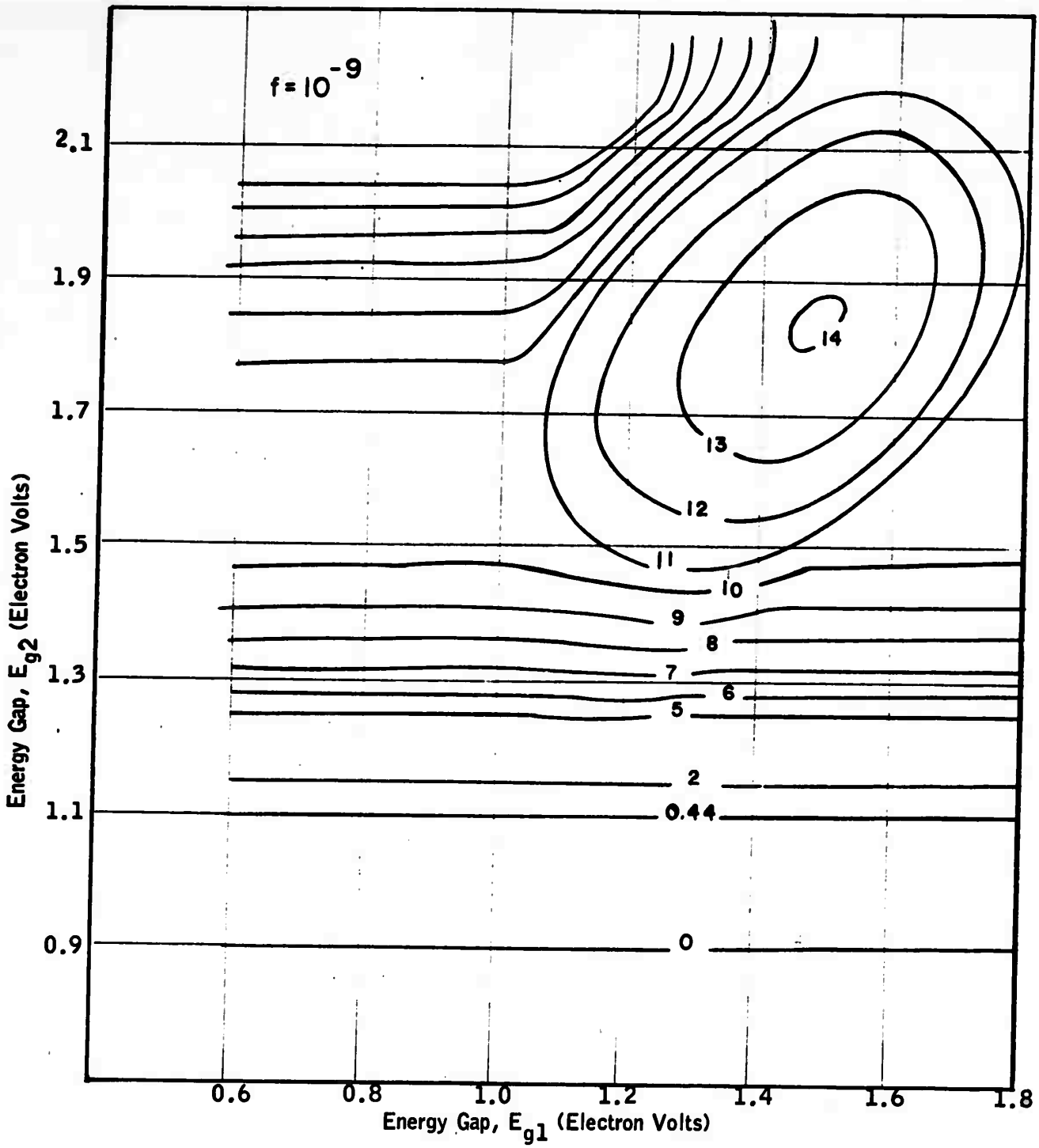

FIG. 8. EFFICIENCY CONTOURS FOR COMPOSITE CELL AS A FUNCTION OF ENERGY GAPS. $f=10^{-9}$.

efficiency of the composite cell is reduced. Further, the optimum energy gaps are shifted to higher values. This latter result is to be contrasted with that of Fig. 5, where it was indicated that lower energy gaps were desirable on the basis of the assumption that $I_o = \exp(-E_g/2kT)$. The maximum efficiency of a single solar cell is also included in Table I, with the corresponding energy gap, in order that a comparison may be drawn between the efficiency of composite cells and single cells. It is seen that the composite cell efficiency is significantly higher.

Another observation to be made from Figs. 4, 6, 7, and 8 is that the rate of fall off in efficiency becomes more rapid in the low energy gap range as f is reduced, leaving the choice of the optimum energy gaps as critical as in the case with no non-radiative recombinations. For the extreme case of $f = 10^{-9}$, the fall off in efficiency at low values of E_g is exceedingly severe. In no case does the efficiency for a given pair of values E_{g_1} and E_{g_2} and a given value of f exceed that for the same values of E_{g_1} and E_{g_2} and a smaller value of f.

On the basis of the foregoing analysis of the efficiency as a function of energy gap and recombination currents, we may conclude that the optimum energy gaps in the ideal case are 1.12 eV and 1.67 eV, and that these values increase if the ideal situation is not realized. In all cases the efficiency of a reflective composite solar cell is approximately 1.3 times that of a single cell when the optimum energy gaps are chosen and other parameters are considered fixed. Further, it becomes obvious that it is essential to avoid deep trapping levels within the forbidden zone if high efficiency solar cells, single gap or composite, are to be made.

4.1.4 The Optimum Junction Depth, and the Effect of Diffused Layer Resistance on Cell Performance

It was shown in Appendix A of the First Semiannual Report,[9] that the component of current generated by the incident solar radiation and reaching the junction could be written

$$I_L = qN_o \left[\frac{\alpha \exp(-\alpha W_n)}{\alpha + 1/L_n} + \frac{\alpha^2}{\alpha^2 - 1/L_p^2} \left\{ 1 - \left(\frac{W_n}{L_p} \right)^2 - \left(1 + \frac{W_n}{\alpha L_p^2} \right) \exp(-\alpha W_n) \right\} \right] \tag{4-45}$$

Eq. (4-45) does not include space-charge-layer recombination or thermal generation currents. It was derived for the case of a solar cell with a p-type base layer and an n-type surface layer, the p-n junction being at a depth W_n beneath the surface. N_o is the number of incident photons per unit area per unit time, α is the absorption constant of the material, and L_n and L_p are the minority carrier diffusion lengths.

In deriving Eq. (4-45) it was assumed that the junction depth, W_n, was much smaller than the diffusion length of a hole in the n-type surface layer, i.e., $W_n << L_p$. The first term in the equation is the contribution from the p-type base layer, the second is the contribution from the surface layer. As a check on Eq. (4-45), it may be noticed that as the diffusion lengths become very large (all carriers generated reach the junction) the light-generated current becomes qN_o, as it should.

The values of α, L_p, and L_n which are physically realizable in semiconductor materials are such that I_L is always less than qN_o, and it can be seen from Eq. (4-45) that it is desirable to have W_n small. In fact, in addition to the original assumption that $W_n << L_p$, it is desirable to have $W_n < 1/\alpha$ so that the average photon penetration will be to a depth greater than W_n. An increase in α requires that W_n be further reduced.

It is apparent then that the collection of the maximum number of photon-excited carriers requires a shallow junction depth, and indeed the diffusion lengths and absorption constants in semiconductor materials limit W_n to a few microns. A conflicting requirement is imposed upon W_n by the fact that the sheet resistance of the thin surface layer appears in series with the external load, causing some of the light-generated electrical power to be lost as Joule heating in the surface layer. This loss can be kept to a minimum only by making W_n large, or through the use of special contact configurations.

A determination of the optimum junction depth requires a correlation of the variation of junction photocurrent I_L as a function of junction depth with the power lost in the effective diffused layer resistance. When the series resistance is considered, the power delivered to the load is given by

$$P = (V - IR_s)\, I, \tag{4-46}$$

The maximum power occurs when

$$dP = 0 = VdI + IdV - 2IR_s dI$$

or

$$\frac{dI}{dV} = -\frac{I}{V - 2IR_s} \tag{4-47}$$

Using the expression

$$I = I_L - I_o \left(\frac{1}{f} \exp(qV/kT) - 1 \right) \tag{4-48}$$

and following the procedure of Eqs. (4-8) to (4-18), it can readily be shown that the maximum power is given approximately by

$$P_{max} \simeq \frac{kT}{q} I_L \ln \frac{fI_L}{I_o} - I_L^2 R_s \tag{4-49}$$

To correlate this expression with that for I_L, let it be assumed that the cell series resistance R_s is inversely proportional to the junction depth, W_n. Then, as W_n increases, R_s will decrease but as pointed out above, the current I_L will also decrease. Thus there will be an optimum value of the junction depth for maximum power output.

The equation for the junction photocurrent is much too unwieldy to permit a straightforward optimization, but it is possible to make approximations which lead to useful results. In particular, it can be shown that the junction photocurrent is given approximately by

$$I_L \simeq A\exp(-W_n/L_p) \tag{4-50}$$

where A is a constant, or at most very slowly varying. If we assume further that W_n is of the same order of magnitude as L_p, then Eq. (4-50) can be approximated as

$$I_L \simeq \frac{A\,L_p}{eW_n} \ . \tag{4-51}$$

Substituting this value of I_L into Eq. (4-49) for the power output of a cell,

$$P_{max} = \frac{M\,A\,L_p}{eW_n} - \frac{C}{W_n}\left(\frac{A\,L_p}{eW_n}\right)^2 \tag{4-52}$$

where

$$M = \frac{kT}{q}\ln\frac{fI_L}{I_o} \ ,$$

and the parameter $C = R_s W_n$ relates the series resistance of the cell to the junction depth. C is a function of the shape of the cell and

of the contact configuration. Treating M as a constant in maximizing Eq. (4-52), the maximum occurs when

$$\frac{W_n}{L_p} = \left(\frac{3CA}{MeL_p}\right)^{1/2} \tag{4-53}$$

Typical values of the parameters in a good silicon cell are $C = 5 \times 10^{-4}$ ohm-cm, $A = 5 \times 10^{-2}$ amperes, $M = 0.5$ volts, and $L_p = 10^{-3}$ cm. For these values W_n/L_p is about 0.2, or the optimum junction depth is approximately 0.2 diffusion lengths or 2.0 microns.

Inserting Eq. (4-53) for the junction depth into Eq. (4-52), one obtains for the maximum power:

$$P_{max} = \frac{2\sqrt{3}}{9}\left(\frac{M^3 AL_p}{eC}\right)^{1/2} \tag{4-54}$$

This equation suggests that, for the values of the parameters used above, a silicon cell should produce about 30 mw/cm^2 output power. This corresponds to an efficiency of 21 percent, surely optimistic but near enough to the experimentally determined values to confirm the validity of the approximations used.

Finally, from Eq. (4-54), it is seen that the maximum power varies as the 3/2 power of M, where

$$M = \frac{kT}{q} \ln \frac{fI_L}{I_o} \tag{4-55}$$

Since $I_o = I_F \exp(-E_g/kT)$ we may write

$$M = \frac{kT}{q} \ln \left[\frac{fI_L}{I_F} \exp (E_g/kT)\right] \tag{4-56}$$

$$= \frac{kT}{q}\left[\ln \frac{fI_L}{I_F} + E_g/kT\right] \tag{4-57}$$

Therefore it may be estimated that the maximum power varies approximately as the 3/2 power of E_g.

This result will cause the values of the optimum energy gaps in a composite cell to be somewhat higher if the internal series resistance is appreciable. For example, it was shown in Section 4.1.2 that, on the basis of spectral efficiency only, the optimum energy gaps were 0.73 eV and 1.46 eV. Following the same procedure as in Section 4.1.2, it can be shown that it is desirable to maximize

$$E_{g_1}^{3/2}\left(E_{g_2} - E_{g_1}\right) + E_{g_2}^{3/2}\left(2.2 - E_{g_2}\right). \tag{4-58}$$

The equations for a maximum are readily found to be

$$\left.\begin{aligned} \frac{3}{2} E_{g_2} E_{g_1}^{1/2} - \frac{5}{2} E_{g_1}^{3/2} &= 0 \\ E_{g_1}^{3/2} + 3.3\, E_{g_2}^{1/2} - \frac{5}{2} E_{g_2}^{3/2} &= 0 \end{aligned}\right\} \tag{4-59}$$

for which $E_{g_1} = 0.95$ eV and $E_{g_2} = 1.6$ eV.

We may conclude that the consideration of the effect of junction depth on the light-generated component of the junction current and on the internal series resistance of the cell requires that the junction depth be approximately one-fourth of the minority carrier diffusion length if the output power is to be a maximum. Further, the reduction in load voltage caused by the internal series resistance of the cell shifts the optimum energy gaps to somewhat greater values.

4.2 Experimental Development of the Composite Solar Energy Converter

4.2.1 Selection of Materials

The foregoing analysis of composite energy gap solar cells on the basis of spectral efficiency, recombination-generation currents, and electrical conversion efficiency has predicted the optimum energy gaps for the two semiconducting materials to be used in a two-element composite cell. It was shown that for the ideal case of no non-radiative recombinations the optimum energy gaps are approximately 1.1 eV and 1.6 eV. It is clear that the values of the two energy gaps are mutually dependent.

Given the values of the energy gaps, the choice of materials then becomes strictly limited, and it is apparent that silicon, in its advanced state of development, is the first choice for the lower energy gap component of the composite cell.

Two materials were considered for the higher energy gap component of the composite cell, namely aluminum antimonide and cadmium selenide. The first of these materials, AlSb, has an energy gap of 1.57 eV,[6] while the same property in CdSe is found to be 1.72 eV.[19]

It was decided to attempt to grow both AlSb and CdSe in single crystal form with most of the effort being directed toward the preparation of the aluminum antimonide. There were two reasons for emphasizing AlSb, rather than CdSe. In the first instance, AlSb is more amenable to conventional Czochralski growth techniques, whereas CdSe, since it sublimes, must be grown either by vapor phase techniques or under high pressures. Secondly, the available data on CdSe indicate that junction formation in this material is more difficult than in the case of AlSb. Thus Shilliday, et. al.,[20] did not observe p-type conductivity in CdSe when the same impurities were used as had been employed in doping CdTe to p-type. The activation energies of

p-type impurities in CdTe are in the range 0.2 to 0.6 eV, and the failure to observe p-type conductivity in CdSe might be explained by the high impurity activation energies which are probably involved.

For these reasons it was decided to concentrate most of the experimental effort on AlSb. Replies to inquiries directed to outside vendors indicated that no single crystal AlSb with proper resistivity and mobility values for solar cell fabrication was commercially available, and the preparation of the material was undertaken in these laboratories. This is discussed in Section 4.2.2 below, while CdSe is discussed in Section 4.2.3.

4.2.2 Preparation of Aluminum Antimonide

The relatively slow development of device-quality compound semiconductors can be attributed to the difficulty of purifying the constituent elements or the compounds themselves. In the case of AlSb several investigators [21, 22] have produced material of high resistivity by means of compensation, but although this provides useful optical samples, the carrier mobilities are invariably low.

Allred, et. al.,[23] have found that the major p-type impurity in AlSb can be reduced by the relatively simple procedure of vacuum-baking the aluminum prior to forming the compound. By this method they produced material with mobilities as high as 400 $cm^2/v\text{-}sec$ and carrier concentrations of the order of $10^{16}/cm^3$. This approach was adopted in these laboratories and polycrystalline ingots of AlSb were grown by the Czochralski method in a modified vacuum furnace described below.

4.2.2.1 Crystal Pulling Furnace

The furnace, shown diagrammatically in Fig. 9, consists essentially of a water-cooled stainless steel bell-jar (a) with a tantalum heating element (b) centrally positioned

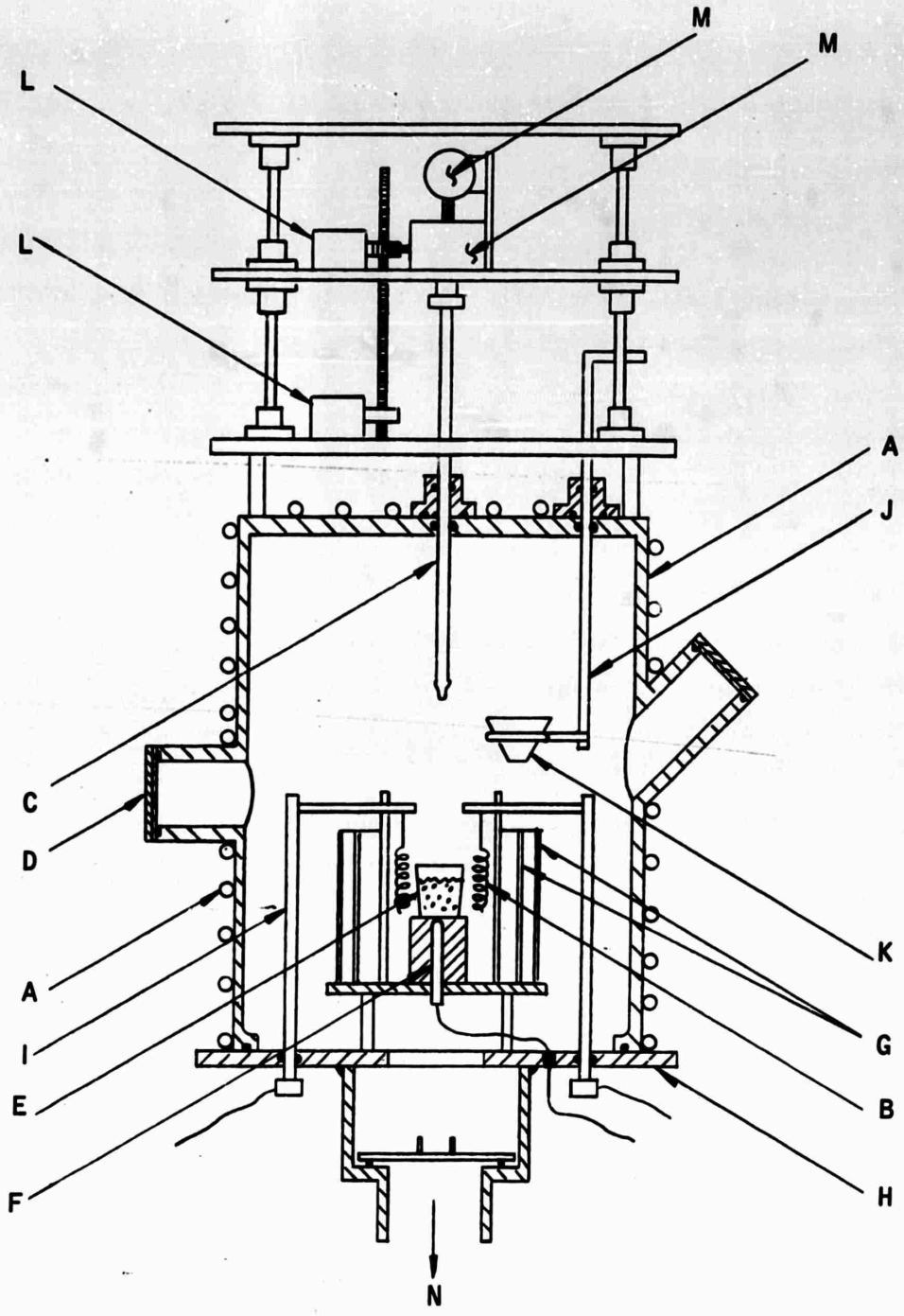

FIG. 9 DIAGRAM OF CZOCHRALSKI PULLING FURNACE

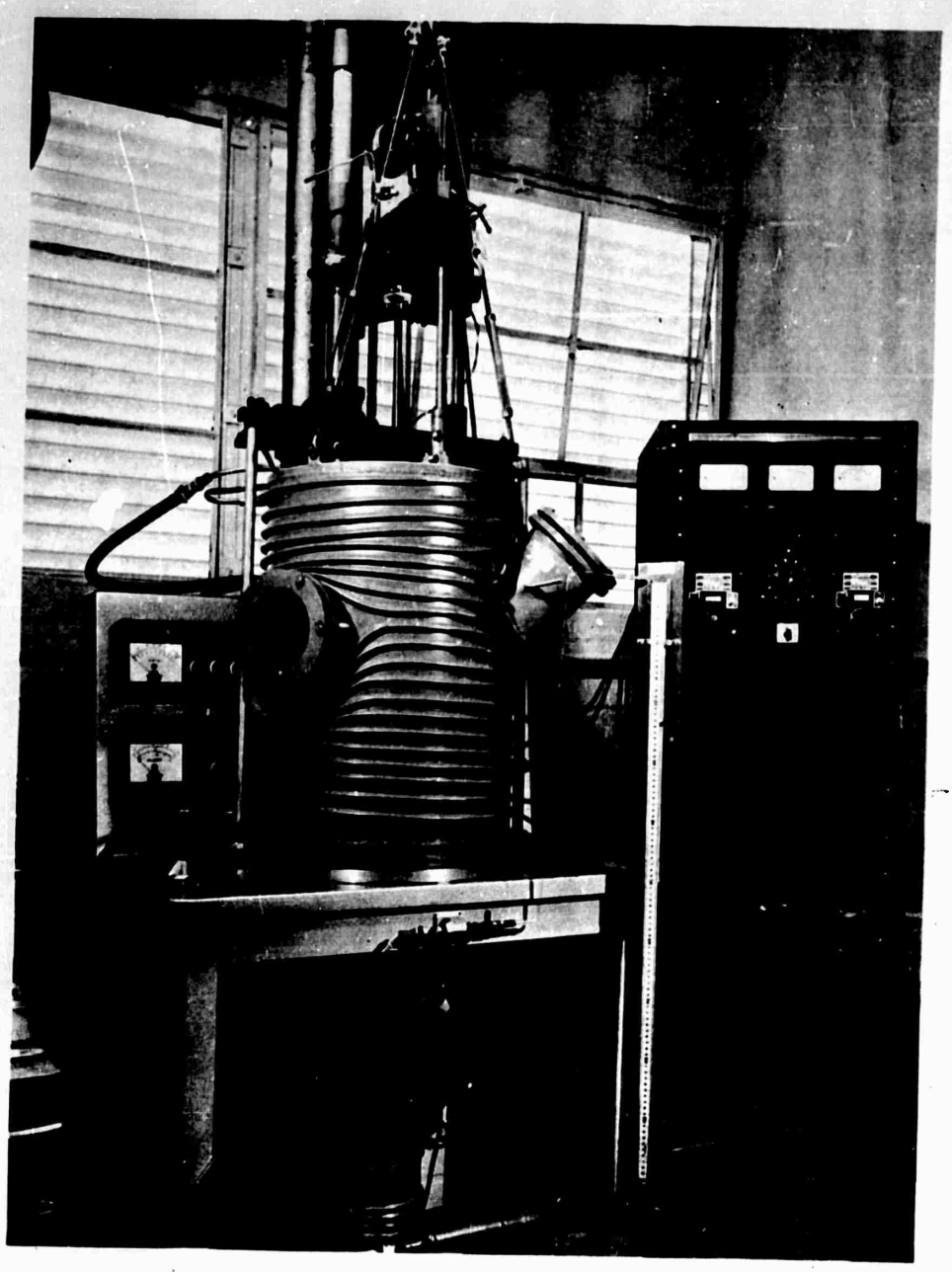

FIG. 10 CZOCHRALSKI FURNACE

under the stainless seed holder (c). Two viewing ports (d) in the wall of the bell-jar permitted full observation of the growing crystal. An alundum crucible (e) was used, and a thermocouple (f) was positioned at the bottom center of the crucible. Two tantalum radiation shields (g) were employed to reduce the heat losses.

Argon, used as a cover gas in growing the AlSb, was admitted through an inlet (not shown) in the base plate (h). The electrical feed-throughs (i) were of stainless steel.

It was necessary to avoid opening the system to add the antimony after the vacuum-baking of the aluminum, and a second stainless steel rod (j) was inserted through a vacuum seal in the top of the bell-jar to satisfy this requirement. This rod, which could be hand rotated, has a stainless extension ring affixed to its lower end, and an alundum filter cone (k) rests in the ring and holds the antimony during the heat treatment of the aluminum. The vertex of the alundum cone was ground away to provide a hole through which the antimony could flow when molten.

The seed holder was raised or lowered at varying rates with two variable speed D.C. motors (l) and associated gearboxes situated above the bell-jar. These operate on a lead screw to achieve the vertical motion. Similarly, a variable speed D.C. motor (m) and reduction gearbox provided for rotation of the seed holder. A liquid-nitrogen-trapped oil diffusion pump (n) enabled a vacuum of 3×10^{-5} mm Hg to be attained. The apparatus is shown pictorially in Fig. 10.

4.2.2.2 Starting Materials

Semiconductor grade antimony was acquired from Ohio Semiconductors, Inc., and this was used without further purification. High purity aluminum, however, is not readily obtainable, and the highest purity material available from Aluminum Corporation of America was used.

The aluminum as received from ALCOA contained significant amounts of both oxygen and magnesium, the latter being an acceptor in AlSb. Since the vapor pressure of magnesium is considerably higher than that of aluminum, 300 mm compared to one micron at 1000°C, it is possible to remove the magnesium by heat-treatment in vacuum at 1000°C for 20 hours. Both aluminum and antimony were etched to remove oxide layers from their surfaces prior to weighing. A solution of 95 percent phosphoric acid and 5 percent nitric acid was found satisfactory for etching the aluminum, and the antimony was etched in CP-4.

4.2.2.3 Crystal Growth

Sufficient quantities of aluminum and antimony to form an ingot of approximately 160 grams were carefully weighed in stoichiometric proportion on an analytical balance. The aluminum was placed in the alundum crucible, and the antimony in the alundum cone, after which the system was closed and evacuated to a pressure of 10^{-4} mm Hg. The cone bearing the antimony was rotated out of the hot zone, to remain in contact with the water-cooled steel wall of the bell-jar during the heat-treatment of the aluminum.

The temperature was then raised to 1000°C, and upon melting, a dull layer of foreign material appeared on the surface of the molten aluminum. It was initially believed, following Allred, et. al.,[23] that this layer was composed chiefly of Al_2O_3. This statement is open to question however, since the oxide, if it were initially distributed throughout the aluminum, should sink to the bottom on melting, being more dense. Aluminum forms a series of complex oxides of low density in combination with hydrogen and carbon, and one or more of these may be present in the floating surface layer. Whatever the contaminant, it is successfully removed from the surface of the melt by continued heat-treatment in vacuum for 20 hours, after which time the surface appears very bright and clean, free of the nucleation centers which would prevent single crystal growth. The

mechanism by which the surface layer is removed is not understood; if a complex oxide is involved it may decompose, the volatile constituents being driven off. Close observation seems to support this view, in that the later stages of the heat-treatment are characterized by a drifting of the remaining scum toward the crucible wall, where the contaminant then appears to sink. This observation is difficult to carry out, however.

As mentioned previously, the volatile magnesium is also removed from the aluminum melt by the heat-treatment, and upon completion of this process the vacuum valves were closed and argon admitted to the system to a pressure just below one atmosphere. This pressure is required to prevent loss of the high-vapor-pressure antimony. The stainless steel ring supporting the antimony-bearing cone was then rotated until the cone was immediately above the crucible. The antimony (melting point 530°C) melted readily and flowed through the hole at the vertex of the cone into the molten aluminum. The temperature was raised to 1065°C, five degrees above the melting point of AlSb. A period of two hours was allowed for the reaction to take place and equilibrium to be attained.

Since an AlSb seed was not available the initial attempts were made with a quartz tube, 2 mm bore, inserted in the seed holder. The quartz tube was wetted by the AlSb when lowered into the melt, and capillary action forced the molten AlSb up the tube. It was hoped that the AlSb would freeze out in the capillary as a single crystal, but the results were invariably polycrystalline. It has since been learned that some difficulty is encountered when an AlSb seed is used, in that the seed becomes coated with an oxide layer during the heat-treatment of the aluminum. This results in nucleation centers which prevent the initiation of single crystal growth.

A seed was fabricated from AUC graphite in the hope of circumventing these difficulties. Oxide layers did not form on the graphite seed, and it was found that the surface of the melt remained much cleaner when the graphite was lowered into it than when a quartz tube was used. To insure adhesion of the AlSb to the graphite seed, two narrow circumferential grooves were machined in the tip of the seed. It was not expected that the initial growth would be monocrystalline; the simple process of necking down was employed in attempts to achieve single crystal growth.

A rotation rate from 8 to 12 RPM was used, and pulling rates of one inch per hour. All of the ingots grown during the contract were polycrystalline, and it was found that the material tends to twin frequently during growth. Sufficient progress toward single crystal ingots in the proper resistivity range to warrant solar cell fabrication was not achieved. Resistivities were in the range from .002 ohm-cm to lower values, too low for solar cells. The material as grown was invariably p-type, the residual impurity of importance probably being magnesium.

4.2.3 Cadmium Selenide

In accord with the intention to investigate cadmium selenide as a possible material for the higher-energy-gap component of the composite solar cell, a furnace was constructed for the growth of single crystals of this material. The method adopted for crystal growth was that used previously by Hammond[24] of Harshaw Chemical Co. and Shiozawa of Clevite Research Laboratories. In this method a pre-doped and sintered slug of CdSe is ground with a mortar and pestle and placed in the inner quartz tube of the growth furnace. The latter is shown diagrammatically in Fig. 11. One end of the charge extends to within four inches of the seed plate, and the other end is backed with a quartz wool plug. A second quartz wool plug is used at the open end of the tube to prevent back diffusion

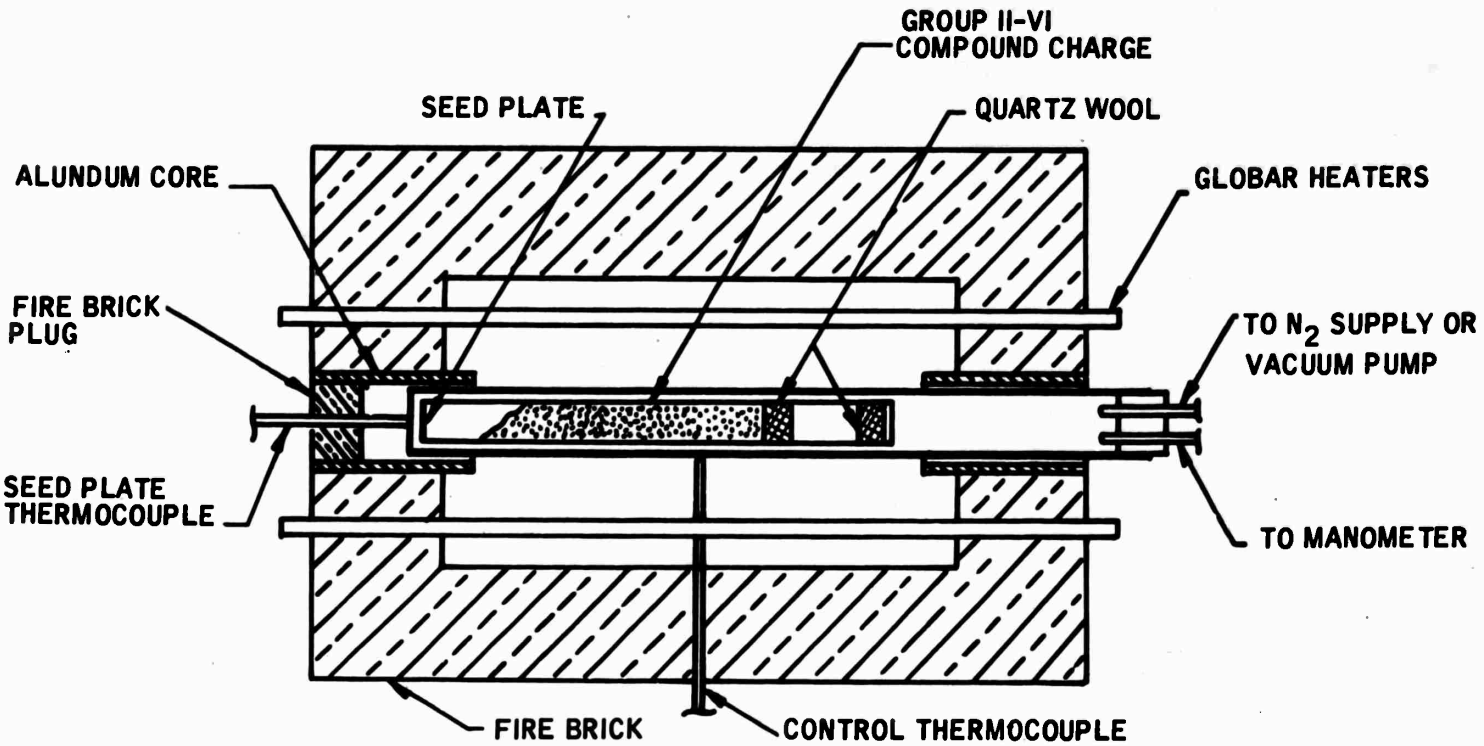

FIG. 11 GROWTH FURNACE DESIGN (AFTER HAMMOND)

of the CdSe vapors. The seed plate, fused to the tube, is polished quartz.

A two-hole rubber stopper is inserted into one end of the outer alundum protection tube, the other end of which is closed. One outlet through the stopper leads to a manometer, and the other to a nitrogen supply and roughing pump. The system is evacuated and flushed with nitrogen several times, and finally filled with nitrogen and sealed.

The temperature is raised until the central hot zone of the furnace is above the temperature required for sublimation of the CdSe, and the expanding nitrogen gas escapes through the manometer. The tube is positioned so that the seed plate temperature is just low enough to permit condensation of the CdSe. The initial material deposited in this process is polycrystalline, but when allowed to continue three to four days, large crystals are obtained at the tail of the ingot.

The central heating chamber of the furnace was cast from ''Super Furnas-Crete'' refractory castable cement. Six silicon carbide heating elements, 38'' in length and 3/4'' in diameter, with an active heating zone 18'' in length, were used as a heat source. The six elements were connected in a series-parallel circuit, two elements in each of three parallel branches. Two grades of firebrick were used for thermal insulation, refractory brick being used in the high-temperature region adjacent to the heating chamber, and a more insulating brick being used in the outer layer.

Operating temperatures of the furnace are in the range from 800° to 1400°C, and power comsumption is 7.5 kilowatts. Temperature control is achieved by means of a Leeds-Northrup Speedomax H C.A.T. temperature controller, magnetic amplifier, and saturable reactor.

Delays (3 1/2 months) in the delivery of the control equipment and alundum tube, plus the fact that most of the effort was directed toward the development of aluminum antimonide, precluded experimental work on CdSe.

4.2.4 Experimental Investigation of a Composite CdS-Si Photovoltaic Solar Energy Converter

It was shown theoretically in the First Semiannual Report[9] that cadmium sulfide is not one of the two ideal materials for a two-element composite solar cell. Nevertheless, the availability of CdS solar cells warranted an experimental determination of the power output of a CdS-Si composite cell compared with that of a Si cell alone, and these measurements serve to verify the theoretical conclusion. The CdS cell employed in the experiments was one of two obtained from the Eagle-Picher Laboratories through the courtesy of W. E. Medcalf of that organization and D. O. Reynolds of WADD. It has an effective area of one cm^2. The Si cell was purchased from the Hoffman Semiconductor Division and is approximately two cm^2 in area.

4.2.4.1 Current-Voltage Characteristics of CdS and Si Cells

Preliminary measurements of the current-voltage characteristics of the CdS and Si cells were made indoors using a tungsten light source and a water filter. Measurements were subsequently taken outdoors, and these are described in detail below.

On 23 January 1960 the sky in the Pasadena area was unclouded, the atmosphere was clear of smog, and it appeared that weather conditions were almost ideal for solar cell measurements in sunlight. At noon the incident solar power, measured with an Eppley pyrheliometer, was 88.5 mw/cm^2. This measurement was made

with a blackened collimating tube mounted over the pyrheliometer to eliminate off-axis radiation.

Repeated measurements of the incident solar power over a period of one hour showed only a slight change, and during this interval the I-V characteristics of the CdS and Si cells were recorded with a Moseley x-y recorder. The results are shown in Fig. 12.

The curves were recorded in a manner which serves to provide information regarding the maximum power which can be obtained from the CdS or Si cells independently, and that which might be obtained from the two cells in a composite reflection-type cell. It will be recalled that a reflection-type cell is one wherein the two elements are mounted at right angles to each other, with a dichroic mirror interposed between the two at an angle of 45°, as indicated in Fig. 1. Numerical calculations given in Ref. 9 serve to indicate that the reflection-type cell is more efficient than the stacked or layered configuration.

The upper curve in Fig. 12 is the I-V characteristic of the Si cell alone, with the solar energy normally incident. The corresponding curve for the CdS cell is labelled "CdS direct incidence." To obtain the I-V characteristics of the two cells under the conditions of composite reflection-cell operation, the dichroic mirror was placed in front of the Si cell at an angle of 45° to the plane of the cell, and the I-V characteristic recorded under the conditions of selective transmission of the mirror. The light reflected by the mirror was normally incident on the CdS cell, the characteristic of the latter also being recorded. Electrical connection was not made to the two cells simultaneously; rather, the measurements were independent.

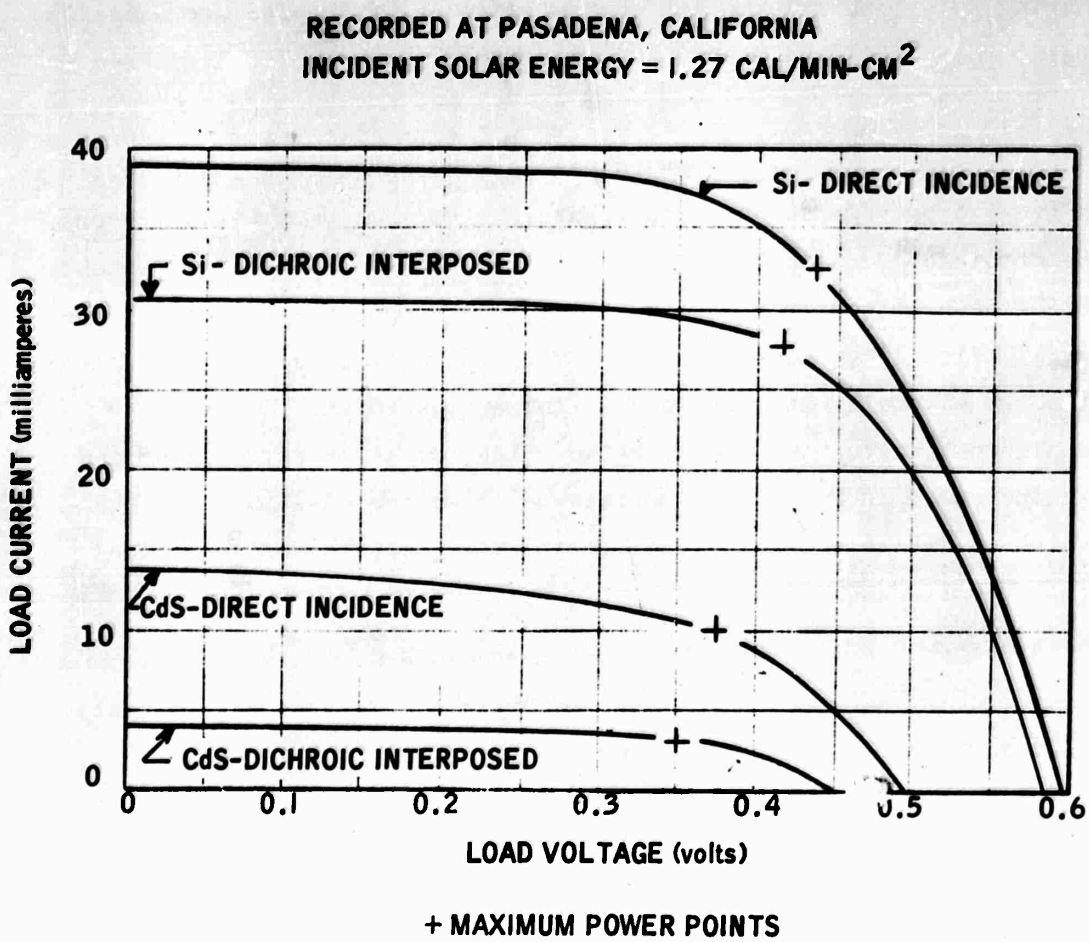

FIG. 12 CURRENT-VOLTAGE CHARACTERISTICS OF CdS AND Si SOLAR CELLS.

Since the measurements taken in conjunction with the dichroic mirror are independent, a single current-voltage characteristic for a composite cell is not shown. However, the curves labeled "dichroic interposed," Fig. 12, allow a determination to be made of the maximum power which can be obtained from each of the two cells under the conditions of composite cell operation. The maximum power points are indicated on each of the four characteristics, and the calculated values are given in Table II. It should be remembered that the Si cell is two cm^2 in area, while the CdS cell is but one cm^2. The results in Table II are normalized to an area of two cm^2.

TABLE II

Maximum Power

Si cell	14.4 milliwatts
CdS cell	7.5 "
Si cell, composite operation	11.4 "
CdS cell, composite operation	2.4 "

The composite cell, if the two elements were connected in parallel, would give an output of less than 13.8 mw since the open circuit voltages and internal impedances of the CdS and Si elements are unlike. Circulating currents would reduce the available power from the value indicated by a simple summation of the independent measurements. Moreover, even independent use of the two elements permits a total maximum power of only 13.8 mw, which must be compared with the 14.4 mw obtainable from the Si element alone when the latter is used without a dichroic mirror in the path of the radiation. Clearly, this composite cell compares unfavorably with Si solar cells.

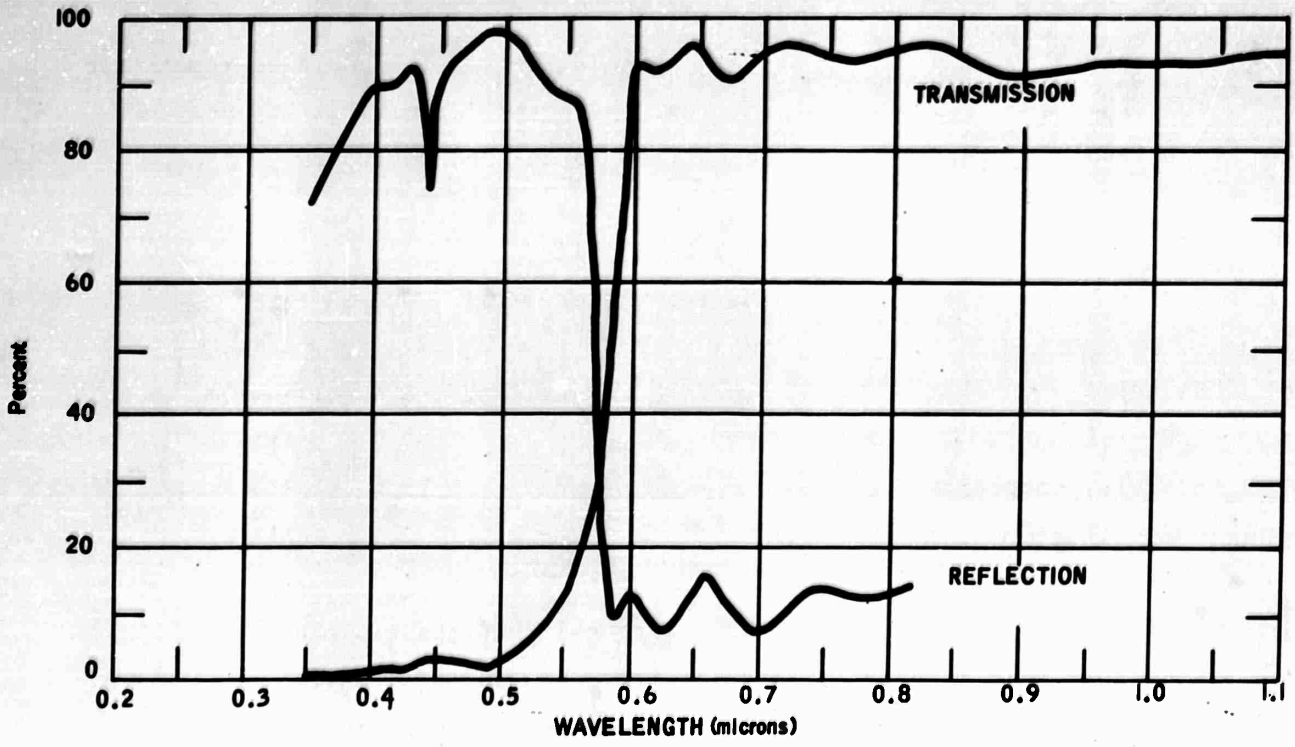

FIG. 13 TRANSMISSION-REFLECTION CHARACTERISTICS OF DICHROIC MIRROR

The dichroic mirror used in these experiments is that described in Ref. 9. Its optical characteristics are given in Fig. 13. In view of the fact that the photovoltaic response of CdS occurs largely in the spectral region beyond the cutoff wavelength,[24] the dichroic mirror used does not split the incident light beam at the optimum wavelength. From the standpoint of increasing the output of the CdS cell, it would be better to utilize a mirror which would split the beam at a somewhat longer wavelength, perhaps 0.9 microns. But this would seriously reduce the output of the Si cell. The difficulty here lies in the fact that the CdS behaves much as a cell with a band separation of 1.3 eV. This is much too close to the energy gap of Si to permit employing these two materials in a composite cell. On the other hand, the intrinsic gap of CdS, 2.4 eV, is too high.

In considering the directions which future experimentation should follow, it should be pointed out that the CdS cell used in this experiment is one of the most efficient fabricated to date. When used without a collimating tube, this cell gave a conversion efficiency of 5.0 percent. The silicon solar cell efficiency is approximately 11.0 percent. Because of the results of the theoretical analysis, namely that the optimum energy gaps are 1.1 and 1.6 eV, and the result of the above experiment, no further work with CdS was carried on.

REFERENCES

1. Cummerow, R. L., Phys. Rev., 95, 16 (1954).
2. Rittner, E. S., Phys. Rev., 96, 1708 (1954).
3. Prince, M. B., J. Appl. Phys., 26, 534 (1955).
4. Loferski, J. J., J. Appl. Phys., 27, 777 (1956).
5. Queisser, H. J., and Shockley, W., "Theoretical Aspects of the Physics of Solar Cells," presented at the American Rocket Society Space Power Systems Conference, Santa Monica, Calif., September, 1960.
6. Blunt, R. F., Hosler, W. R., and Frederikse, H.P.R., Phys. Rev., 96, 571 (1954); Phys. Rev., 96, 576 (1954); Phys. Rev., 96, 578 (1954).
7. Folberth, O. G., and Oswald, F., Z. Naturforsch, 9a, 1050 (1954).
8. Jenny, D. A., and Braunstein, R., J. Appl. Phys., 29, 596 (1958).
9. Burns, J. W., Evans, W., and Armstrong, H., First Semiannual Report, "Investigation of Composite or Stacked Variable Energy Gap Photbvoltaic Solar Energy Converter," USASRDL Contract DA 36-039 SC 85244, 8 Jan 1960.
10. Johnson, F. S., J. Meteorol., 11, 431 (1954).
11. Shive, J. N., Proc. Inst. Radio Engrs., 40, 1410 (1952).
12. Rappaport, P., Phys. Rev., 93, 246 (1954).
13. Pfann, W., and van Roosbroeck, W., J. Appl. Phys., 25, 1422 (1954).
14. Shockley, W., Bell System Tech. J., 28, 435 (1949).
15. Kittel, C., "Introduction to Solid State Physics" (John Wiley and Sons, New York, 1953), 2nd Ed., pg. 350.
16. Kleinknecht, H., and Seiler, K., Z. Physik, Bd 139, 599 (1954).

17. Hall, R. N., Proc. Inst. Radio Engrs., 40, 1512 (1952).

18. Sah, C., Noyce, R. N., and Shockley, W., Proc. Inst. Radio Engrs., 45, 1228 (1957).

19. Bube, R. H., Phys. Rev., 98, 431 (1955).

20. Shilliday, T. S., Harman, T. C., Genco, J. I., and Logan, M. J., Second Quarterly Progress Report, "Studies, Research, and Investigations on Compounds Formed from Elements of Groups II and VI" (October, 1957), AD 156572.

21. Herczog, A., Haberecht, R. R., and Middleton, A. E., J. Electrochem. Soc., 105, 533 (1958).

22. Kover, F., "Electrical and Optical Properties of Aluminum Antimonide," International Conference on Solid State Physics in Electronics and Telecommunications, Brussels (June, 1958).

23. Allred, W. P., Mefferd, W. L., and Willardson, R. K., J. Electrochem. Soc., 107, 117 (1960).

24. Hammond, D. A., Shirland, F. A., and Baughman, R. J., Final Report, "A Cadmium Sulfide Solar Generator" (December, 1957), AD 151036.

5. CONCLUSIONS

The analysis of composite energy gap solar cells on the basis of spectral efficiency, saturation current, and recombination current has predicted the optimum energy gap semiconductor materials to be used in such cells. In the case where non-radiative recombinations in the space charge layer are kept to a minimum, the optimum energy gaps are approximately 1.1 electron volts and 1.65 electron volts. These values become somewhat higher if the fraction of non-radiative recombinations is large, being approximately 1.5 eV and 1.85 eV in the extreme case.

According to the analysis, the maximum efficiency which may be expected from a composite cell is 32.5 percent, and this may be compared with the maximum of 24.5 percent expected from a single solar cell on the same analysis. These figures are for the ideal case of no non-radiative recombinations, and the analysis shows that such recombinations can seriously reduce the efficiency. The current technology of silicon solar cells yields cells with 15 percent efficiency at best. The analysis indicates that the non-radiative recombination rate yielding this efficiency for silicon is such that if the technologies of materials with energy gaps of 1.25 eV and 1.7 eV were as advanced as that of silicon, the efficiency of a composite cell fabricated from these materials would be 25 percent. The results given above are for air mass zero, corresponding to the region above the Earth's atmosphere but in the vicinity of the Earth.

The choice of materials to satisfy the energy gap requirements remains as critical when the non-radiative recombination rate is high as it is in the ideal case. In the latter situation, silicon is the

optimum material for the lower-energy-gap component of the composite cell, and aluminum antimonide is a potentially promising material for the higher-energy-gap component.

The device construction and electrical efficiency analysis shows that the optimum depth of the p-n junction in a solar cell is approximately one-fourth of the diffusion length of the diffused layer minority carrier.

Further analysis of the device design shows that a reflection type of composite cell which is not limited by absorption of low energy photons in the higher-energy-gap component is more efficient than a transmission type cell in which the components are stacked one above the other.

Aluminum antimonide holds great promise for the high-energy-gap component of a composite solar cell, and since this material is not commercially available, continued efforts should be directed toward its preparation and evaluation. It was found that aluminum as received from the vendors was not of sufficient purity to be used without further purification, but that the requirement of high-purity could be approached by a vacuum heat-treatment of the aluminum prior to forming the compound. Crystals of the compound could then be pulled by the Czochralski method under a pressure of one atmosphere of argon.

Another possible material for the high-energy-gap component of the solar cell is cadmium selenide. Since this material sublimes it is not amenable to Czochralski growth; high pressures would be necessary to melt the compound. However, this difficulty may be obviated by growing single crystals of the material from the vapor phase. Although a furnace was constructed for the latter purpose, the decision to concentrate most of the experimental effort on AlSb curtailed the investigation of CdSe.

One of the theoretical results presented in the First Semiannual Report, namely that cadmium sulfide would not suffice as one of the two materials in a composite solar cell, was verified experimentally. Measurements in sunlight indicated that a composite cell fabricated from CdS and Si elements was not as efficient as the Si cell alone.

The results presented in this report indicate that the experimental investigation of AlSb should be continued. The future development of a satisfactory composite cell depends upon the successful preparation of suitably doped single crystals of this compound or of another high mobility 1.7 eV energy gap semiconductor material.

6. OVERALL CONCLUSIONS

The essential conclusions which may be drawn from this work are as follows:

1) For air mass zero, when non-radiative recombinations occurring in the space charge layers of the p-n junctions of the cells are minimized, the theoretical optimum energy gaps for the semiconductor materials in the composite cell are 1.1 eV and 1.65 eV.

2) The theoretical composite cell efficiency in the above case is 32.5 percent, compared with 24.5 percent for a single solar cell.

3) As the rate of non-radiative recombination in the space charge layers increases, the optimum energy gaps also increase, and the efficiency is reduced. In an extreme case, the band gaps are 1.45 eV and 1.85 eV, and the efficiency 14 percent.

4) The optimum composite cell is 1.3 times as efficient as the best single cell and the composite solar cell is potentially (theoretically) useful to that extent only.

5) The optimum junction depth in a solar cell is 0.25 times the diffusion length of the minority carrier in the surface layer.

6) The choice of the optimum semiconductors in the case of severe non-radiative recombination is as critical as in the ideal case.

7) In the ideal case, silicon is the optimum material for the lower-energy-gap component of the composite cell, and aluminum antimonide holds promise for the higher-energy-gap component.

8) The reflection type of composite cell is more efficient than the transmission type.

9) A suitable high-energy-gap semiconductor material must be prepared and an efficient p-n junction solar cell fabricated from that material before useful direct experimental verification of these predictions can be made in sunlight. (A silicon-germanium composite cell was proposed early in this program and was dropped as non-responsive to the actual solar spectrum. The silicon-germanium composite cell would be useful to demonstrate the composite cell principle using a slightly cooler spectrum since both materials are well developed in the semiconductor art.)

7. RECOMMENDATIONS

The analysis given in this report indicates that the compound semiconductor aluminum antimonide could very probably be one of the two optimum materials for the composite solar cell. Furthermore, the work of Loferski[4] in 1956 indicated that a single aluminum antimonide solar cell should by itself be more efficient than the silicon solar cells commonly in use (also predicted in radiationless recombination theory). For these reasons it is felt that further experimental investigation and development of aluminum antimonide, and of AlSb solar cells, should prove fruitful.

Since it has been shown that the theoretical efficiency of a composite solar cell can be 1.3 times that of single cells, it is recommended that experimental determinations of composite cell efficiencies be made subsequent to the necessary development work on AlSb.

It was suggested during the negotiations for the contract work herein described that it would be instructive to conduct a laboratory experiment in which the temperature of the entire system was scaled downward. Thus one might use an artificial light source of color temperature 3700°K, and a composite solar cell at the temperature of dry ice. The optimum energy gaps of the semiconductors used in the components of the composite cell in such a system would be 0.75 eV and 1.1 eV, and the obvious choices would be germanium and silicon. Since these materials are already in a highly developed state, little effort would be required to demonstrate the feasibility, or lack of same, of a composite cell. Since the two materials, Ge and Si, are not optimum for a composite cell for extra-terrestrial operation, this experiment was not carried out during the contract. Such an experiment would be informative, however.

8. BIBLIOGRAPHY

The bibliography is in three sections, and the references in each are listed chronologically. The first section pertains to the photovoltaic effect and solar cells, the second to aluminum antimonide, and the third to cadmium selenide. Standard handbooks and textbooks are not included. See also the REFERENCES at the end of Section 4.

8.1 The Photovoltaic Effect and Solar Cells

1. E. Becquerel, "On Electric Effects Under the Influence of Solar Radiation," Compt. rend., 9, 561 (1839).

2. W. G. Adams and R. E. Day, "The Action of Light on Selenium," Proc. Roy Soc., A25, 113 (1877).

3. B. Lange, "New Photoelectric Cell," Z. Physik, 31, 139 (1930).

4. W. Schottky, "Cuprous Oxide Photoelectric Cells," Z. Physik, 31, 913 (1930).

5. L. O. Grondahl, "The Copper-Cuprous Oxide Rectifier and Photoelectric Cell," Revs. Modern Phys., 5, 141 (1933).

6. F. Eckart and A. Schmidt, "Distribution of Spectral Sensitivity of Selenium Barrier Layer Photocells," Z. Physik, 118, 199 (1941).

7. K. Lehovec, "The Photovoltaic Effect," Phys. Rev., 74, 463 (1948).

8. M. Tomura, "A Selenium Barrier Layer Photoelement. V," Bull. Chem. Soc. Japan, 22, 52-7 (1949). (CA 44:29g)

   See also, "A Selenium Barrier Layer Photoelement. VI," Bull. Chem. Soc. Japan, 22, 145-8 (1949). (CA 45:32g)

9. W. Ehrenberg, C. Lang, and R. West, "The Electron Voltaic Effect," Proc. Phys. Soc., 64, 424 (1951).

10. R. N. Hall, "Electron-Hole Recombination in Germanium," Phys. Rev., 87, 387 (1952).

11. W. Shockley and W. T. Read, Jr., "Statistics of the Recombinations of Holes and Electrons," Phys. Rev., 87, 835-42 (1952).

12. J. N. Shive, "Properties of the M-1740 p-n Junction Photocell," Proc. Inst. Radio Engrs., 40, 1410-13 (1952).

13. R. N. Hall, "Power Rectifiers and Transistors," Proc. Inst. Radio Engrs., 40, 1512-18 (1952).

14. P. Rappaport, "The Electron-Voltaic Effect in p-n Junctions Induced by Beta-Particle Bombardment," Phys. Rev., 93, 246-7 (1954).

15. D. M. Chapin, C. S. Fuller, and G. L. Pearson, "A New Silicon p-n Junction Photocell for Converting Solar Radiation into Electrical Power," J. Appl. Phys., 25, 676 (1954).

16. H. Kleinknecht and K. Seiler, "Single Crystals and Crystals with p-n Junctions of Silicon," Z. Physik, 139, 599-618 (1954).

17. D. C. Reynolds and G. Leies, "Light Converted into Electricity with Cadmium Sulfide Crystal," Elec. Eng., 73, 734 (1954).

18. R. L. Cummerow, "Photovoltaic Effect in p-n Junctions," Phys. Rev., 95, 16-21 (1954).

19. R. L. Cummerow, "Use of Silicon p-n Junctions for Converting Solar Energy to Electrical Energy," Phys. Rev., 95, 561-2 (1954).

20. W. G. Pfann and W. van Roosbroeck, "Radioactive and Photoelectric p-n Junction Power Source," J. Appl. Phys., 25, 1422-34 (1954).

21. D. C. Reynolds, G. Leies, L. L. Antes, and R. E. Marburger, "Photovoltaic Effect in Cadmium Sulfide," Phys. Rev., 96, 533 (1954).

22. D. C. Reynolds and S. J. Czyzak, "Mechanism for Photovoltaic and Photoconductivity Effects in Activated CdS Crystals," Phys. Rev., 96, 1705 (1954).

23. E. S. Rittner, "Use of p-n Junctions for Solar Energy Conversion," Phys. Rev., 96, 1708 (1954).

24. R. Gremmelmaier, "GaAs Photocells," Z. Naturforsch., 10a, 501-2 (1955). (PA 58:9666)

25. R. H. Bube, "Temperature Dependence of the Width of the Band Gap in Several Photoconductors," Phys. Rev., 98, 431-3 (1955).

26. M. B. Prince, "Silicon Solar Energy Converters," J. Appl. Phys., 26, 534 (1955).

27. J. J. Loferski and P. Rappaport, "Electron Voltaic Study of Electron Bombardment Damage and Its Thresholds in Ge and Si," Phys. Rev., 98, 1861 (1955).

28. "Proceedings of the International Conference on Peaceful Uses of Atomic Energy," (1955).

29. "Transactions of the Conference on the Use of Solar Energy," Univ. of Arizona Press (1955).

30. P. Rappaport, J. J. Loferski, and E. G. Linder, "The Electron-Voltaic Effect in Germanium and Silicon p-n Junctions," RCA Review, XVII, 100 (1956).

31. D. A. Jenny, J. J. Loferski, and P. Rappaport, "Photovoltaic Effect in GaAs p-n Junctions and Solar Energy Conversion," Phys. Rev., 101, 1208 (1956).

32. J. J. Loferski, "Theoretical Considerations Governing the Choice of the Optimum Semiconductor for Photovoltaic Solar Energy Conversion," J. Appl. Phys., 27, 777 (1956).

33. M. Cutler and H. M. Bath, "Surface Leakage Current in Silicon Fused Junction Diodes," Proc. Inst. Radio Engrs., 45, 39 (1957).

34. C. Sah, R. N. Noyce, and W. Shockley, "Carrier Generation and Recombination in p-n Junctions and p-n Junction Characteristics," Proc. Inst. Radio Engrs., 45, 1228 (1957).

35. M. Wolf, "Design of Silicon Photovoltaic Cells for Special Applications," AIEE-IRE Semiconductor Devices Conference, Boulder, Colo. (1957).

36. R. E. Halstead, "Temperature Considerations in Solar Battery Development," J. Appl. Phys., 28, 1131 (1957).

37. S. G. Ellis, F. Herman, E. E. Loebner, W. J. Merz, C. W. Struck, and J. G. White, "Photovoltages Larger Than the Band Gap in ZnS Crystals," Phys. Rev., 109, 1860 (1958).

38. M. Wolf and M. B. Prince, "New Developments in Silicon Photovoltaic Devices and Their Application in Electronics," International Conference on Solid State Physics in Electronics and Telecommunications, Brussels (June, 1958).

39. R. Gremmelmaier, "Irradiation of p-n Junctions with Gamma Rays: A Method for Measuring Diffusion Lengths," Proc. Inst. Radio Engrs., 46, 1045 (1958).

40. M. B. Prince and M. Wolf, "New Developments in Silicon Photovoltaic Devices," J. Brit. Inst. Rad. Engrs., 18, 583 (1958).

41. J. J. Loferski and P. Rappaport, "The Effect of Radiation on Silicon Solar Energy Converters," RCA Review, XIX, 536 (1958).

42. B. Goldstein and L. Pensak, "High Voltage Photovoltaic Effect," J. Appl. Phys., 30, 155 (1959).

43. P. Rappaport, "The Photovoltaic Effect and Its Utilization," RCA Review, XX, 373 (1959).

44. Y. A. Vodakov, G. A. Lomakina, G. P. Naumov, and Y. P. Maslakovets, "A p-n Junction Photocell Made of Cadmium Telluride," Soviet Phys.-Solid State, 2, 1 (1960), and "Properties of p-n Junctions in CdTe Photocells," Soviet Phys.-Solid State, 2, 11 (1960).

45. M. Wolf, "Limitations and Possibilities for Improvement of Photovoltaic Solar Energy Converters," Proc. Inst. Radio Engrs., 48, 1246 (1960).

46. J. J. Wysocki and P. Rappaport, "Effect of Temperature on Photovoltaic Solar Energy Conversion," J. Appl. Phys., 31, 571 (1960).

47. H. J. Queisser and W. Shockley, "Some Theoretical Aspects of the Physics of Solar Cells," American Rocket Society Space Power Systems Conference, Santa Monica, Calif. (Sept., 1960).

8.2 Aluminum Antimonide

48. H. Gautier, Contrib. à l'Etude d'alliages, 112 (1901).

49. W. Campbell and J. Matthews, "The Alloys of Aluminum," J. Am. Chem. Soc., 24, 253-266 (1902).

50. G. Tammann, Z. anorg. u. allgem. Chem., 48, 54 (1906).

51. E. A. Owen and G. D. Preston, "The Atomic Structure of Two Intermetallic Compounds," Proc. Phys. Soc. (London), 36, 341-8 (1924). (CA 18:3502)

52. W. Guertler and A. Bergmann, "Ternary System: Aluminum-Antimony-Magnesium," Z. Metallkunde, 25, 81-4, 111-16, 132 (1933).

53. G. Tammann and A. Ruhenbeck, "Disintegrating Intermetallic Compounds," Z. anorg. u. allgem. Chem., 223, 288-96 (1935). (CA 29:7207[1])

54. K. Lohberg, "The Corrosion of Intermetallic Compounds," Z. Metallkunde, 41, 56-9 (1950). (CA 44:4852i)

55. H. Welker, "On New Semiconducting Compounds," Z. Naturforsch., 7a, 744-9 (1952).

56. R. K. Willardson, A. C. Beer, and A. E. Middleton, "Some Electrical Properties of Aluminum Antimony," Bull. Am. Phys. Soc., 28, 42 (March, 1953); Phys. Rev., 91, 243 (1953).

57. E. Justi and G. Lautz, "The Electrical Behavior of AlSb," "Abhandl. Braunschweig. wiss. Ges., 5, 36-47 (1953). (PA 57:1296)

58. R. G. Breckenridge, "Semiconducting Intermetallic Compounds," Phys. Rev., 90, 488-9 (1953). (CA 47:90936)

59. H. Welker, "New Semiconducting Compounds," Z. Naturforsch., 8a, 248-51 (1953).

60. "Semiconducting Intermetallic Compounds," National Bur. Stds., Tech. News Bull., 37, 174-5 (1953).

61. R. Gremmelmaier and O. Madelung, "Preparation of Single Crystals of Semiconducting Compounds of the Type A^{III}-B^{V}," Z. Naturforsch., 8a, 333 (1953). (CA 47:11871g)

62. R. F. Blunt, H.P.R. Frederikse, J. H. Becker, and W. R. Hosler, "Electrical and Optical Properties of Intermetallic Compounds. III, AlSb," Phys. Rev., 96, 578-80 (1954). (CA 49:2861b)

63. R. K. Willardson, A. C. Beer, and A. E. Middleton, "Electrical Properties of Semiconducting AlSb," J. Electrochem. Soc., 101, 354-8 (1954). (CA 50:52a)

64. W. Sasaki, N. Sakamoto, and M. Kuno, "Some Electrical Properties of Aluminum Antimonide," J. Phys. Soc. Japan, 9, 650-1 (1954). (CA 49:10729h)

65. R. G. Breckenridge, et. al., "On the Intermetallic Compounds InSb, GaSb, and AlSb," Physica, 20, 1073-6 (1954). (PA 58:3766)

66. E. W. Saker and F. A. Cunnell, "Intermetallic Semiconductors," Research, 7, 114-20 (1954).

67. C.H.L. Goodman, "Semiconducting Compounds and the Scale of Electronegativities," Proc. Phys. Soc. (London), 67B, 258-9 (1954).

68. H. Welker, "Semiconducting Intermetallic Compounds," Physica, 20, 893-909 (1954)

69. F. Oswald and R. Schade, "Determination of the Optical Constants of Type A^{III}-B^{V} Semiconductors in the Infrared," Z. Naturforsch., 9a, 611-17 (1954). (CA 49:511)

70. F. A. Cunnell, F. T. Edmond, and J. L. Richards, "Measurements on Some Semiconducting Compounds with the Zincblende Structure," Proc. Phys. Soc. (London), 67B, 848-9 (1954). (CA 49:1423e)

71. H. B. Briggs, R. F. Cummings, H. J. Hrostowski, and M. Tannenbaum, "Optical Properties of Some Group III-Group V Compounds," Phys. Rev., 93, 912 (1954).

72. G. Wolff, P. H. Keck, and J. D. Broder, "Preparation and Properties of III-V Compounds," Phys. Rev., 94, 753 (1954).

73. H. J. Hrostowski and M. Tannenbaum, "Recent Work on Group III Antimonides and Arsenides," Physica, 20, 1065 (1954).

74. C.H.L. Goodman, "Bond Relationships in Diamond-Type Semiconductors," J. Electronics, 1, 115-21 (1955).

75. H.P.R. Frederikse and R. F. Blunt, "Photoeffects in Intermetallic Compounds," Proc. Inst. Radio Engrs., 43, 1828-35 (1955). (CA 50:3069b)

76. F. Herman, "Speculations on the Energy Band Structure of Zincblende Type Crystals," J. Electronics, 1, 103-114 (1955).

77. H. Pfister, "Cleavage of A^{III}-B^{V} Compounds InSb and AlSb," Z. Naturforsch., 10a, 79 (1955).

78. A. R. Regel and M. S. Sominskii, "The Effect of Impurities on the Mechanism of Electrical Conductivity of AlSb," Zhur. Tekh. Fiz. (USSR) 25, 768 (1955).

79. F. Oswald, "Optical Determination of the Temperature Dependence of Band Gaps of Semiconductors of the Type A^{III}-B^{V}," Z. Naturforsch., 10a, 927-30 (1955).

80. K. Smirous, "The Influence of Impurities on the Properties of Aluminum Antimonide," Czechoslov. J. Phys., 6, 299-300 (1956). (PA 60:370)

81. A. Abraham, "Photoelectric Properties of AlSb," Czechoslov. J. Phys., 6, 624 (1956). (CA 9295g)

82. F. Kover and A. Quilliet, "Electrical and Optical Properties of Aluminum Antimonide. Action of Lithium," Compt. rend., 244, 1739 (1957). (CA 51:10993c)

83. W. P. Allred, B. Paris, and M. Genser, "Zone Melting and Crystal Pulling Experiments with AlSb," J. Electrochem. Soc., 105, 93 (1958).

84. F. J. Reid and R. K. Willardson, "Carrier Mobilities in InP, GaAs, and AlSb," J. Electronics and Cont., 5, 54-61 (1958). (PA 63:6993)

85. H. A. Schell, "Single Crystals and p-n Layer Crystals From Aluminum Antimonide," Z. Metallkunde, 49, 140 (1958). (CA 52:10725b)

86. F. Kover, "On the Electrical and Optical Properties of Aluminum Antimonide," International Conference on Solid State Physics in Electronics and Telecommunications, Brussels (June, 1958).

87. A. Herczog, R. R. Haberecht, and A. E. Middleton, "Preparation and Properties of Aluminum Antimonide," J. Electrochem. Soc., 105, 533 (1958).

88. I. I. Burdiyan and A. S. Borshchevskii, "The Preparation and Some Properties of Solid Solutions in the System AlSb-GaSb," Zhur. Tekh. Fiz. (USSR), 28, 12 (1958).

89. A. C. Beer, "Semiconducting Compounds - A Challenge in Applied and Basic Research," J. Electrochem. Soc., 105, 743-751 (1958).

90. D. N. Nasledov and S. V. Slobodchikov, "Electric and Thermoelectric Properties of Aluminum Antimonide," Zhur. Tekh. Fiz. (USSR), 28, 715 (1958).

91. D. N. Nasledov and S. V. Slobodchikov, "Electrical Properties of n-type AlSb," Soviet Phys. - Solid State, 1, 748 (1959). (PA 64:598)

92. I. I. Burdiyan and B. T. Kolomiets, "A Study of the Conductivity and the Hall Effect in Solid Solutions of the AlSb-GaSb System," Soviet Phys. - Solid State, 1, 1165 (1959).

93. I. I. Burdiyan, "Some Additional Information Regarding Solid Solutions in the AlSb-GaSb System," Soviet Phys. - Solid State, 1, 1360 (1959). (PA 63:6381)

94. W. P. Allred, W. L. Mefferd, and R. K. Willardson, "The Preparation and Properties of Aluminum Antimonide," J. Electrochem. Soc., 107, 117-122 (1960).

95. R. H. Wieber, H. C. Gordon, and C. S. Peet, "The Diffusion of Copper into AlSb," J. Appl. Phys., 31, 608 (1960).

8.3 Cadmium Selenide

96. M. Chikashige and R. Hikosaka, "Metallographic Investigation of the System Cadmium-Selenium," Mem. Coll. Sci., Kyoto Imp. Univ., 2, 239-44 (1917).

97. M. L. Huggins, "Crystal Structures of Some Sulfides, Selenides, and Tellurides," Phys. Rev., 21, 211-2 (1923). (CA 18:2984^5)

98. W. Zachariasen, "The Crystal Structures of the Selenides of Beryllium, Zinc, Cadmium, and Mercury," Z. Physik. Chem., 124, 436-49 (1926). (CA 21:1210)

99. L. S. Mathur, "Determination of the Latent Heats of Vaporization of the Selenides of Cd, Hg, and Telluride of Zn from Absorption Spectra of their Vapors," Indian J. Phys., 11, 177-85 (1937). (CA 31:7736^3)

100. E. C. Pitzer and N. E. Gordon, "Hydrolytic Precipitation of Cadmium Selenide from Seleno-Sulfate Solutions," Ind. Eng. Chem., 10, 68-9 (1938). (CA 32:2458^3)

101. N. E. Gordon and E. C. Pitzer, "Cadmium Selenide (Method of Production)," U. S. Patent 2,176,495 (Oct. 17, 1939). (CA 34:P1137^6)

102. T. Asai, "Photoconductivity of Semiconducting Layers of Heavy Metal Sulfide or Selenide. I. The Relation between the Spectral Sensitivity and the Light Absorption in the Photoconductive Layer of Cadmium Selenide, and the Microscopic Examination of Its Structure in Relation to Its Photoconductivity," Bull. Inst. Phys. Chem. Res. (Tokyo), 19, 1-3 (1940). (CA 34:4983^1)

103. H. Wolff, "Secondary Electrons from Highly Photoelectric Semiconductors," Ann. Physik, 39, 591-603 (1941). (CA 36:4408[9])

104. L. Wesch, "Newer Results with Lenard Phosphors," Reichsant Wirtschaft-susbau, Chem. Ber. Pruf.-Nr. 15, 487-501 (1942). (CA 41:5023a)

105. R. Frerichs, "The Photoconductivity of Incomplete Phosphors," Phys. Rev., 72, 594-601 (1947). (CA 42:1513cd)

106. B. T. Kolomiets and E. K. Putseiko, "The Valve Photoeffect in Selenium With Admixtures of Cadmium," Zhur. Eksp. i Teoret. Fiz., 17, 818-23 (1947). (CA 43:4102g)

107. P. Gorlich and J. Heyne, "A New Photoresistance Cell for the Visible Region of the Spectrum," Optik, 4, 206-12 (1948). (CA 46:8954g)

108. E. K. Putseiko, "Determination of the Sign of the Carriers of Photoelectric Current by the Condenser Method," Doklady Akad. Nauk, SSSR, 67, 1009-12 (1949). (CA 43:8896a)

109. J. Yamaguchi and S. Katayama, "Cadmium Selenide on Selenium Rectifiers," J. Phys. Soc. Japan, 5, 386-7 (1950).

110. E. Schwarz, "Photoconductive Cells of Cadmium Selenide," Proc. Phys. Soc. (London), 63B, 624-5 (1950).

111. J. W. Earley, "Description and Synthesis of the Selenide Minerals," Amer. Mineral., 35, 337-64 (1950). (CA 45:71f)

112. K. Schubert, "Crystal Structure," Z. Naturforsch., 5a, 345-6 (1950). (CA 44:9764a)

113. S. Nagata and K. Agata, "Crystal Structure of Cadmium Selenides of Selenium Rectifiers," J. Phys. Soc. Japan, 6, 523-4 (1951).

114. E. Schwarz, "Photoconductive Cells of Cadmium Selenide," Proc. Phys. Soc. (London), 64B, 821-2 (1951).

115. A. N. Arsen'eva-Geil, "External Photoelectric Effect in Semiconductors," Izvest. Akad. Nauk, SSSR, Ser. Fiz. 16, 122-8 (1952). (CA 46:9413e)

116. H. C. Jensen and R. J. Cashman, "Distribution of Trapping Levels in CdSe," Phys. Rev., 96, 798-9 (1954).

117. H. J. Dirksen and W. Memelink, "Photoconductivity in Cadmium Selenide," Appl. Sci. Res., 4, 205-16 (1954). (PA 58-957)

118. D. A. Jenny and R. H. Bube, "Semiconducting Cadmium Telluride," Phys. Rev., 96, 1190-1 (1954).

119. E. W. Saker and F. A. Cunnell, "Intermetallic Semiconductors," Research, 7, 114-20 (1954).

120. R. H. Bube, "Infrared Quenching and a Unified Description of Photoconductivity Phenomena in CdS and CdSe," Phys. Rev., 99, 1105-15 (1955).

121. M. Aoki and S. Tanaka, "Crystal Structure and Physical Properties of CdSe," Oyo Butsuri, 24, 113-17 (1955). (CA 49:15458c)

122. K. Hauffe and H. G. Flint, "On the Electrical Conductivity of Cadmium Selenide," Ann. Physik, 15, 141-7 (1955). (PA 58:3748)

123. R. H. Bube, "Temperature Dependence of the Width of the Band Gap in Several Photoconductors," Phys. Rev., 98, 431-3 (1955).

124. R. H. Bube, "Photoconductivity of the Sulfide, Selenide and Telluride of Zinc or Cadmium," Proc. Inst. Radio Engrs., 43, 1836-50 (1955).

125. F. Herman, "Speculations on the Energy Band Structure of Zincblende Type Crystals," J. Electronics, 1, 103-14 (1955). (PA 59:2544)

126. D. M. Heinz and E. Banks, "Growth and Some Properties of a Large Single Crystal of Cadmium Selenide," J. Chem. Phys., 24, 391-8 (1956). (PA 59:2536)

127. G. B. Abdullaev, "Electronographic Investigation of Structure of Blocking Layer in Selenium Rectifiers," Izvest. Akad. Nauk, Azverbaidzhan SSR, 4 (1956).

128. P. F. Browne, "Luminescence of the Sulfide Phosphors," J. Electronics, 2, 154-66 (1956). (CA 51:17341)

129. M. A. Talibi, G. B. Abdullaev, and Z. A. Aliyarova, "The Effect of Gamma and X-rays on the Photoconductivity of Polycrystalline Cadmium Selenide," (1956). (CA 51:11053a)

130. S. Pakswer and C. S. Szegho, "Sintered Cadmium Sulfide and Cadmium Selenide Photocells," Proc. Natl. Electronics Corp., 12, 669-76 (1956). (CA 51:11843a)

131. B. T. Kolomiets and S. G. Pratusevich, "Photoresistor Made of Cadmium Selenide," Radiotekh. i Elektron, 1, 1174-6 (1956). (CA 51:12640d)

132. S. A. Semiletov, "Electronographic Investigation of the Structure of Thin Layers of CdS, CdSe, and CdTe," Kristallografiya, 1, 306-10 (1956).

133. V. A. Kotovich and V. A. Frank-Kamenetskii, "Standard X-ray Diagrams of Several Selenides, Tellurides, and Arsenides of Copper, Silver, Zinc, Cadmium, Gallium, and Indium," Ucheneya Zapiski, Leningrad, Gasudarst, Univ. in A. A. Zhdanova, Ser. Geol. Nauk, 8, 135-36 (1957). (CA 52:19329f)

134. R. H. Bube, "Oxygen Sorption Phenomena on Cadmium Selenide Crystals," J. Chem. Phys., 27, 496-500 (1957).

135. N. A. Tolstoi and J. A. Sakalov, "Luminescent and Photoelectric Properties of Polycrystalline Cadmium Selenide," Optika i Spektroskopiya, 3, 495-503 (1957). (CA 52:4331h)

136. "Zinc, Cadmium, and Zinc-Cadmium Selenides and Tellurides," British patent 786,310 (1957). (CA 52:P4121e)

137. H. Tubota, "Diffusion Potential of Selenium Rectifiers," Mem. Fac. Sci., Kyushu Univ., Ser. B, 2, 95-7 (1957). (CA 52:8740g)

138. I. Kasabow and D. Mikhailova, "Dynamic Characteristics of Selenium Rectifiers Containing a Deposited Layer of Cadmium Selenide," Compt. rend. Acad. Bulga. Sci., 10, 181-4 (1957). (CA 52:14342h)

139. E. F. Gross and V. V. Sobolev, "Exciton Absorption and Emission Spectra in Cadmium Selenide Crystals," Soviet Phys.-Tech. Phys., 1, 1580-1 (1957). (CA 51:17415b)

140. S. V. Svechnikov, "Peculiarities in the Photoconductivity of Cadmium Selenide," Zhur. Eksp. i Teoret. Fiz., 34, 548-54 (1958). (CA 52:9778b)

141. R. H. Bube and L. A. Barton, "Some Aspects of Photoconductivity in Cadmium Selenide Crystals," J. Chem. Phys., 29, 128-37 (1958). (CA 52:17979a)

142. N. I. Vitrikhovskii and N. I. Nitsetskaya, "Preparation of CdS-CdSe Monocrystals from Vapor Phase and Some of Their Properties," Fiz. tverdogo Tela, 1, 397-402 (1959). (PA 63:7957)

143. V. A. Dorin, B. I. Kuzuretsov, and D. N. Nasledov, "Studies of the Growth of an n-type Semiconductor Layer at the Contact of Cadmium With Selenium," Fiz. tverdogo Tela, 1, 734-9 (1959). (PA 63:602)

144. Li Chzhi-Tszyan, "Electron Energy Dependence of Induced Conductivity of Cadmium Sulfide and Cadmium Selenide Films Bombarded with Slow Neutrons," (Li Chih-Tsien), Fiz. tverdogo Tela, 1, 77-81 (1959). (PA 63:605)

145. U. B. Sultanov and I. G. Prestorononin, "On the Life-Time of Minority Carriers in the Sub-Surface Layer in CdSe+Ag Single Crystals," Fiz. tverdogo Tela, 2, 26-7 (1960). (PA 63:7958)

9. IDENTIFICATION OF KEY TECHNICAL PERSONNEL

The following is a list of the key technical personnel assigned to the contract and taking part in the work covered by this report. Included is the approximate number of hours of work performed by each during the term of the contract.

PERSONNEL	HOURS WORKED
J. W. Burns, Project Supervisor	1376
W. H. Evans, Research Engineer	436
W. V. Wright, Division Manager, Solid State Division	219
I. Weiman, Associate Manager, Solid State Division	154
Total	2185
H. Armstrong, Consultant	48

UNCLASSIFIED